Department of Solid Mechanics, Lund Institute of Technology, Sweden

Stability of the lumbar spine

A study in mechanical engineering

Anders Bergmark

ACTA ORTHOPAEDICA SCANDINAVICA SUPPLEMENTUM NO. 230, VOL. 60. 1989

MUNKSGAARD · COPENHAGEN

Printed in Sweden
Ortonova AB, Lund
Wallin & Dalholm Boktryckeri AB, Lund
1989

Contents

Introduction

The aim of this work was to find the conditions for mechanical stability of the human lumbar spine.

Several models of the back are found in the literature, from the simple force couple model, curved beam models and link systems to two- and three-dimensional finite element models with or without muscles.

In almost every biomechanical textbook, the force couple model of the back is presented (Figure 1). The only (but anyhow very important) question that can be answered by using this model is:

> What are the approximate magnitudes of the compression and shear force in the spine and the tensile force in the back muscles at different loading on the human body at different postures?

The very high compressive force in the spine that is obtained from calculations by means of this model in some loading cases and the fact that the ligamentous spine becomes mechanically unstable for a vertical load of only a fraction of this value (Lucas and Bresler 1961) shows that there must be an active muscle support to the spine acting so as to avoid lateral or sagittal buckling. This is particularly evident for the lumbar spine, since no other elements than the muscles are available for the mechanical support. Consequently the present work is concentrated on the lumbar spine. Furthermore, since the risk of loss of stability appears to be largest at upright standing position under vertical loading, only such loadposture cases are studied. The next question is obvious:

> How is the lumbar spine stabilized by the surrounding muscles?

The complex anatomy of the back, with a multitude of muscles with apparently similar function, raises the next two questions:

> What is the rationale of this complexity?
> How are the muscle forces distributed among the different muscles?

These two latter questions are not necessarily answered by means of mechanical considerations only.

Several models are presented in the literature, which deal with these questions. To be able to handle the complexity of the system, "non-mechanical" force distribution assumptions have been introduced in these models.

By thorough mechanical modeling and using mechanical methods only, it is however possible, to give a more detailed mechanical picture of the spinal system than has been shown before.

The salient features of the work presented here, are the distinction between a local and a global mechanical system of the trunk, the introduction of the stiffness contribution from the activated muscles, and the investigation of the mechanical stability.

A general assumption has been that the spinal system must be mechanically stable in essentially the same way as purely passive engineering structures (*i. e.* structures without controlling servo-mechanisms), namely by possessing stiffnesses that are high enough. This assumption is based on the fact that the spinal system would collapse (buckle) so quickly, if the stiffness needed to maintain stability was significantly reduced, that nerve-muscle control would be too slow for corrections. On the other hand, stiffnesses only somewhat smaller than needed to maintain stability could probably be accepted because attempted buckling would then be slow enough to permit nerve-muscle control of the system configuration. If this is the "strategy" of the system, the region within which

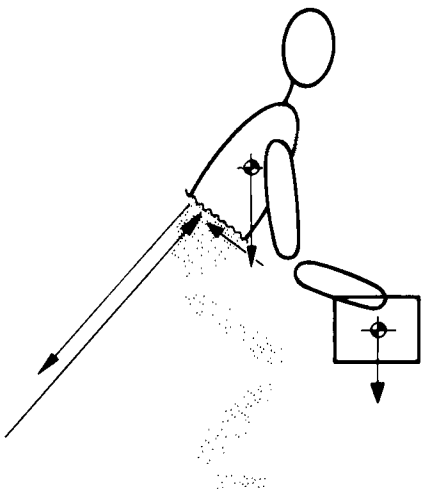

Figure 1. Force couple model of the back.

stability is found to prevail in the present work would be somewhat, but not much, enlarged.

As an introduction for those readers who are not acquainted with mechanical engineering, the first chapter contains a description of the methods used and comments on the conspicuous difference between the muscle-skeletal system and ordinary mechanical structures and the difficulties introduced because of this difference.

A description of the simple force couple model and two complex models presented in the literature is made in Chapter 2.

The statically indeterminate character of the back as a mechanical system, calls for the introduction of additional conditions. Some of these "non-mechanical" but anyhow "mechanically reasonable" principles are presented in Chapter 3.

In order to provide a good base for modeling the spinal system, Chapters 4 and 5 contain a description of the anatomy of the lumbar spine and of the mechanical properties of its different elements.

The division into a local and a global system is introduced in Chapter 5.

Chapters 6 and 7 contain the study of the stability of the lumbar spine. First the concept of mechanical stability is presented by means of an example much simpler than the spinal system. A slight expansion of the simple example leads to a model by which the sagittal stability of the ankle joint is evaluated. The last part of Chapter 6 presents a realistic lumbar spine model.

The numerical results are presented in Chapter 7.

In Chapter 8 these results are compared to the experimental data available notably measurements of trunk muscle electromyography (EMG) and posture. Finally the last three questions raised in this introduction are answered as far as the limited loadcases analysed allow.

It must be poited out, that the term "stability" is often interpreted differently by physicians and physicist.

In mechanics, stability is a well defined concept, namely the ability of a loaded structure to maintain static equilibrium even at (small) fluctuations around the equilibrium position. If stability does not prevail, an arbitrarily small change of the position is sufficient to cause "collapse", *i. e.* the structure moves further away from equilibrium.

For a physician the term "stability" is associated with "clinical stability". According to White and Panjabi (1978) the definition of "clinical stability of the spine" is as follows: "The ability of the spine under physiologic loads to limit patterns of displacement so as not to damage or irritate the spinal cord or nerve roots and, in addition, to prevent uncapacitating deformity or pain due to structural changes. Any disruption of the spinal components (ligaments, discs, facets) holding the spine together will decrease the clinical stability of the spine. When the spine looses enough of these components to prevent it from adequately providing the mechanical functions of protection, measures are taken to reestablish the stability."

In mechanical terms, clinical stability is associated with the magnitude of the deformations when the spine is loaded. Thus the spine can be more or less clinically stable. Clinical stability can therefore be regarded as a continuously variable phenomenon.

Mechanical stability, on the other hand, is not continuously variable. The system is either stable or unstable (in rare cases it is indifferent, *i.e.* neither stable nor unstable).

The material presented here is an abbreviated and slightly revised version of my thesis (Bergmark 1987).

Professor Bertram Broberg has given valuable suggestions on the manuscript. All illustrations were made by mrs. Doris Nilsson.

1. Engineering methods

The equations of equilibrium

For a static mechanical system, the *conditions of equilibrium* must always be fulfilled, *i.e.* the resulting force and the resulting moment acting on the system must be zero. These conditions must be valid for the whole mechanical system as well as for any part of the system.

As an example a simple model will be analysed, viz a forearm subjected to a vertical load acting on the hand (Figure 1-1). Thus the part of the body studied is the forearm and all forces acting on this part must be considered (Figure 1-2). A mechanical term often used to describe such an imaginary isolated system is the "free-body diagram".

The conditions of equilibrium are now applied. Force equilibrium requires that

$$P_{br} - C - F = 0 \qquad (1.1)$$

and moment equilibrium requires that

$$P_{br} \cdot a - F \cdot b = 0 \qquad (1.2)$$

where a and b are the lever arms.

From (1.1) and (1.2) the unknown quantities P_{br} and C can be found. One obtains:

$$P_{br} = F\, b/a \qquad (1.3)$$

$$C = F\,(1 - b/a) \qquad (1.4)$$

The forearm example is a *plane* (two-dimensional) problem. For such a problem, three equations of equilibrium are available. Here only two of them, (1.1) and (1.2) are shown. The result from the horizontal force equilibrium condition gives the simple result that as there is no outer horizontal load, there is no inner horizontal reaction (acting at the elbow joint) either.

In the three-dimensional case, 6 equations of equilibrium are available.

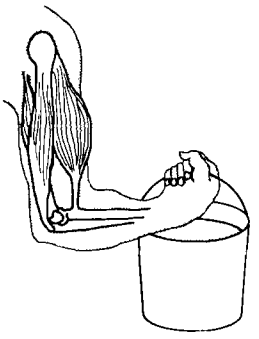

Figure 1-1. Forearm subjected to a vertical load acting on the hand.

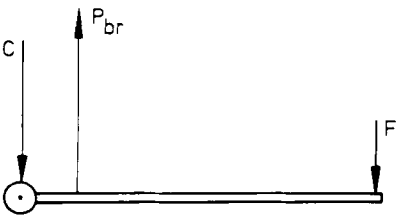

Figure 1-2. The forces acting on the forearm. C: Compressive force from the upper arm acting in the elbow-joint, P_{br}: tensile force in the brachialis muscle and F: outer load. This is the "free-body diagram" of the forearm.

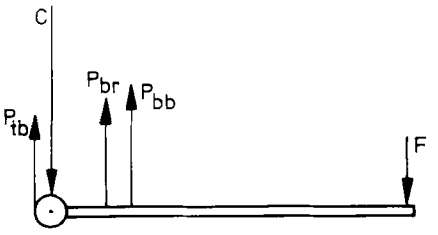

Figure 1-3. Free-body diagram of the forearm when muscle action from the biceps- and the triceps-brachii muscles are added.

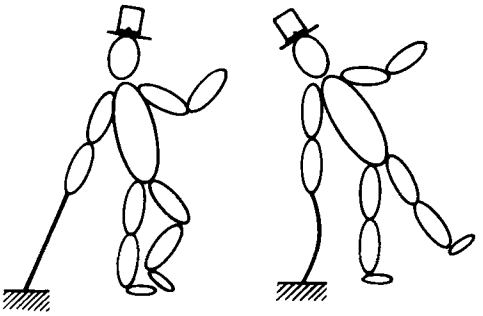

Figure 1-4. A slender rod will loose its mechanical stability if the compressive force exceeds a critical value.

Statically determinate and indeterminate systems

Systems for which the equations of equilibrium are sufficient for determination of the unknown forces are called *statically determinate.*

The brachialis muscle is only one of three main muscles acting over the elbow joint. When the other two, the biceps- and the triceps-brachii muscles, are introduced the free-body diagram will be modified (Figure 1-3). The triceps brachii is antagonistic and the biceps brachii synergistic to the brachialis muscle action over the elbow joint. The forces in the three muscles cannot uniquely be determined by the conditions of equilibrium only. Any combination of the three muscle forces, which counteracts the moment from the outer load is acceptable.

A system in which the equations of equilibrium are not sufficient to determine the forces is called *statically indeterminate.*

In such a system additional rules, beside the conditions of equilibrium, must be introduced to determine the unknown forces.

The collapse of a mechanical system

To avoid collapse of a static mechanical system, satisfaction of the conditions of equilibrium of the system are necessary but not sufficient. In addition *mechanical stability* must be maintained.

A very simple example of this is a slender rod subjected to a compressive force. The straight rod is at equilibrium irrespectivel of the magnitude of the axial load, but looses its mechanical stability (Figure 1-4), if the compressive force exceeds a certain value.

The concept of mechanical stability in general as well as the mechanical stability of the lumbar spine will be discussed in detail in Chapter 6.

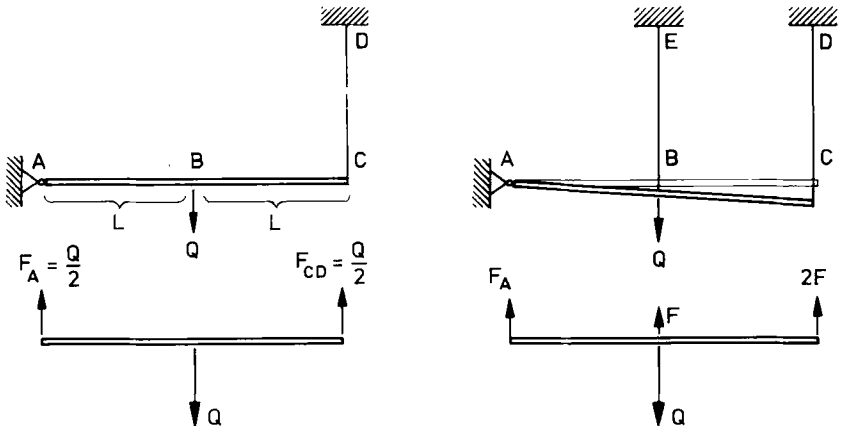

Figure 1-5. To the left: The elastic beam AC and the string CD loaded by a vertical load Q, form a mechanical system. The force in the string CD is obviously Q/2.

To the right: Another string BE (equal to CD) is attached to the system which makes the system statically indeterminate. The assumption that the beam AC is stiff gives the geometrical constraint that the elongation of CD is twice the elongation of BE. Assuming also a linear-elastic string material, *i.e.* for equal transverse areas the force is proportional to the elongation, the free-body diagram shown is obtained. The condition for moment equilibrium around point A gives the equation: $Q \cdot L - F \cdot L - 2F \cdot 2L = 0$ with the solution: $F = Q/5$.

Passive and active components

From a mechanical point of view a distinction between two types of components of a muscle-skeletal system, *passive* respectively *active* components, must be done (Broberg 1981).

Passive components (bony and cartilageous elements, ligaments, tendons and fasciae) are deformed in a way that depends on the forces applied, only.

For active components (muscles) there is no unique relation between the geometrical configuration and the force. Within physiological range, the muscle force is not depending on the muscle length.

A system may be statically indeterminate, without containing active components (Figure 1-5). Then the relation between forces and geometrical configuration can be found by means of the external loads, the force-displacement characteristics of the passive components and the geometrical constraints of the system. This is an ordinary problem for a mechanical engineer and the same theoretical tools are applied for structures made of steel, concrete, wood, bone etc.

For the muscle-skeletal system, on the other hand, the tools introduced for exclusively passive components can no longer be used. Some additional rule regarding the muscle force distribution must be applied.

An important property of a muscle is that its stiffness can be determined for each given force level (Morgan 1977). Thus a muscle can be assigned passive properties for an isometrically contracted (or a relaxed) state. This is important when evaluating the mechanical stability of the spine in a muscle activated state.

Mechanical difference between an active muscle-skeletal system and a passive system

Because of the abundance of active components in the spinal system, both *load* and *posture* must be specified in order to describe unambiguously the case under study. This is in contrast to most engineering situations in which only *either* the load *or* the posture need to be specified (Figure 1-6).

The *posture* (configuration) of the human body can be described by specification of the positions of the skeletal components. For the purpose of an *overall* analysis of the mechanical state resulting from external loading at a fixed posture, these bones can be regarded as stiff (non-deformable) elements. Moreover, also the joints can be regarded as stiff (*i.e.* allowing only rotations), except, of course, in a *detailed* analysis of individual joints, for instance an intervertebral disk.

The description of the posture can be regarded simply as a description of the geometry of the body to be subjected to external loads. Another thing is that different postures imply different internal loads, even if external loads were completely absent. Flexion of the spinal column, for instance, cannot be achieved without muscle forces, because of the bending stiffness of the column (mainly due to the deformation properties of disks and ligaments).

As regards the spinal column itself, with *passive* components like ligaments and articular facets, etc. but without muscles, it would not matter *in principle* whether the posture or the forces were specified, since a one-to-one relation exists between the two.

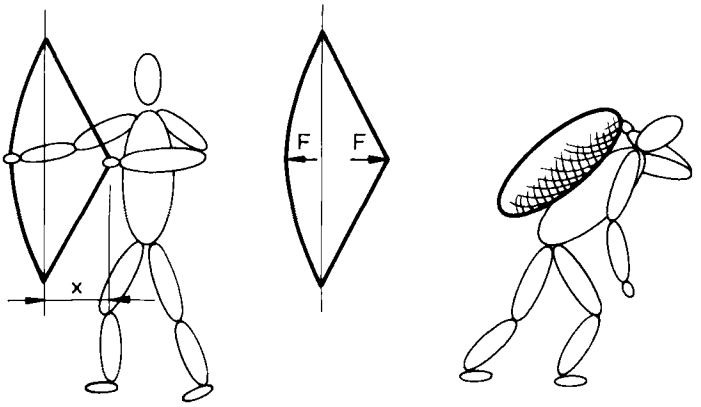

Figure 1-6. To the left: Either the posture (configuration) of the bow *or* the force on the bowstring specifies the mechanical state of the bow uniquely.

To the right: Both force *and* posture must be specified to describe the mechanical state of the body.

2. Models of the human spine

The force couple model

The simplest trunk model is the force-couple model (Figure 2-1).

The forces introduced in the free-body diagram after cutting an imaginary plane through the L3 level are easily calculated provided the moment carried by the spine, including the ligaments (the ligamentous spine) is known. Since this moment is small in the erect and moderately flexed postures it is usually neglected.

The equilibrium equations are:

$$-W - Q + C - E = 0 \quad (2.1)$$

$$-E\,l_e + Q\,l_q + W\,l_w = 0 \quad (2.2)$$

The solutions are:

$$E = Q\,l_q/l_e + W\,l_w/l_e \quad (2.3)$$

$$C = Q(1 + l_q/l_e) + W(1 + l_w/l_e) \quad (2.4)$$

Use of this force couple model gives a good evaluation of the compressive joint forces but the force distribution between different muscles and ligaments carrying the tension force cannot be found.

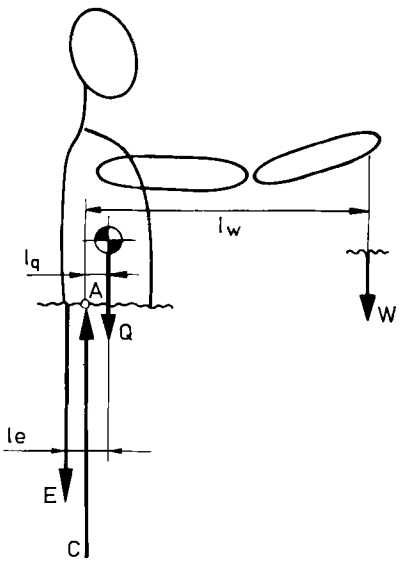

Figure 2-1. Force-couple model of the back. To the right is the free-body diagram of the trunk. A: most anterior disk midpoint, W: weight of outer load, Q: weight of trunk, arms and head, C: compressive force in the spine and E: tension force in the erector spinae muscle. l_w, l_q and l_e are the corresponding lever arms.

Complex models

In order to treat either nonsymmetrical loading cases, which demand separate consideration of muscles in left and right muscle groups, or twisting where a separate consideration of the oblique abdominal muscles in external and internal parts is necessary (or both), a more sophisticated trunk model is needed. Such a model requires for instance more muscles. The number of unknown forces increases rapidly with the sophistication and the model will certainly be statically indeterminate. In the trunk model introduced by Schultz et al. (1982a, b, 1983) only six equations of equilibrium are available (Figure 2-2) while the number of unknown forces is up to 22 (models with different numbers of muscles were used; Schultz et al. 1983). In order to solve the problem, "non mechanical" force distribution laws were introduced. Different rules were used for the calculations (Schultz et al. 1982a) and the

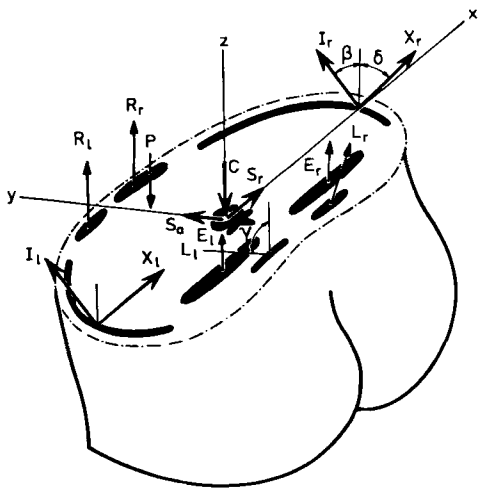

Figure 2-2. Trunk model adapted from Schultz et al. (1983).

muscle forces were compared to results from EMG measurements of the trunk muscle activity. The best correlation between calculated muscle forces and EMG was obtained for the force distribution law based on the assumption that no antagonistic muscle action was present and that the muscle tension in the most loaded muscle was as low as possible (the min-max cost function).

By means of the two models described hitherto, the forces acting on an imaginary plane transverse to the spine can be calculated.

Skogland and Miller (1980) introduced a spinal model including all thoracic and lumbar vertebrae. The properties of the spinal motion segments (*i. e.* two adjacent vertebrae including the intervertebral disk and the ligaments) and in total 146 muscle slips were included. The muscles were treated as "perfect force-sources" and no influence from muscle stiffness was included. The aim of their investigation was to study the mechanical behavior of the spine in connection with scoliosis. Two different force distribution rules were used: minimization of spinal deformation and minimization of the sum of squares of the muscle forces. This last rule works essentially the same way as the min-max cost function used by Schultz et al. (1982a, b, 1983).

3. Models of the control functions

How the central nervous system (CNS) controls trunk muscles during their response to loads at different postures is not sufficiently well understood to permit detailed modeling. More or less mechanically reasonable assumptions about how the different muscles are controled must be introduced.

Any control function assumed must comply with the conditions of equilibrium and mechanical stability in order to avoid mechanical collapse of the muscle-skeletal system. An obvious additional condition is that only tensile muscle forces are available.

No mechanical principle seems to forbid antagonistic muscle action. Such action may well be be accepted and is sometimes even necessary to mechanically stabilize a joint.

The indeterminate nature of the activated muscle-skeletal system can be approached in different ways. Common for them all, is however that a division in functional muscle units must be made first.

Functional muscle units

In order to simplify the analysis of the statically indeterminate system or even in some cases to transform it to a statically determinate one, muscles with equivalent functions are grouped together to functional units. The force couple trunk model where all back muscles are considered as one functional muscle unit is an example of transforming the indeterminate system to a statically determinate one.

From the mechanical point of view, any meaningful division in functional muscle units must be based on the creation of a system capable of maintaining the conditions of equilibrium as well as the conditions of mechanical stability. These constraints determine, not necessarily uniquely, the force distribution between the functional units (Figure 3-1).

Within the units the force distribution is determined by physiological principles, for example fatigue (Crowninshield and Brand 1981, Dul et al. 1984) which demands loadsharing between the synergistic muscles and the successive recruitment of motor units of increasing size for an increased load.

In the trunk force couple model (Figure 2-1) only the conditions of equilibrium are considered. According to measurements of the intradiskal pressure (Andersson et al. 1977, Schultz et al. 1988b) from which the compressive in vivo force in the spine can be evaluated, this model can give a good picture of the joint forces. The force distribution within the erector spinae muscles can, however, not be obtained.

Even if the division of functional muscle units is based on mechanical considerations, the system may still be statically indeterminate. To be able to determine the muscle unit forces, additional conditions must be introduced.

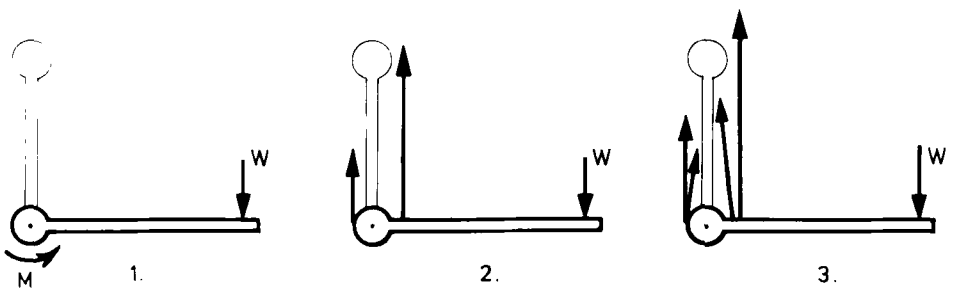

Figure 3-1. Examples of functional muscle units of the elbow joint. 1: All muscles capable to develop the joint torque are grouped together forming a torque functional unit, 2: Two units, one synergistic and one antagonistic and 3: Four units, synergistic and antagonistic single joint units plus synergistic and antagonistic multiple joint units. W: weight carried in the hand.

Optimization

In the statically indeterminate system, an infinite number of different muscle activity patterns can satisfy the mechanical requirements. One useful working hypothesis regarding the selection among the patterns, is that the CNS performs the control in an optimal manner by minimizing some mechanical functional, or cost function, such as maximum muscle stress (force per unit area), spinal shear force, spinal compressive force or displacements of the spine. Also a completely "non-mechanical" functional based on physiological or psychological factors is reasonable.

In the optimization control system, no muscle is allowed to act on its own: every single muscle force is a function of all the others.

A survey of cost functions based on the forces and tensions of the system was presented by Dul et al. (1984), and Skogland and Miller (1980) introduced displacements of the spinal column in their cost function.

Optimization is however not the only way to deal with the indeterminate muscle-skeletal system.

Each muscle king

In the anarchistic control function each muscle is sovereign. The activity in the muscle is only depending on the mechanical state of that muscle, a stretching of the muscle causes increased force and vice versa. A theoretical model of the each muscle king approach, called the "correspondence principle", was presented by Broberg (1981)

In one sense a muscle is always anarchistic. Due to its passive elastic properties, a sudden small stretch will always cause an increased muscle force.

Programs ready made

In a similar way as the motor unit recruitment in the muscle successively involves larger units for an increased load, the onset of the activity in different muscles may follow a given order.

The muscle activity pattern of a given task is determined by the initial conditions identified by neurologic signals and the onset of the muscle activity follows a ready made program. The different parts of the erector spinae muscle may be activated in a given order, for example first the muscles acting between the vertebrae and then other muscles when assistance is demanded.

Combinations

The "real" control function most probably is a combination of the three aforementioned strategies.

The onset of muscle activity is highly correlated to the expected task, which gives a preference for the ready made program approach. In case of uncertainty about the outer load, there will be a general increase of muscle activity in synergistic as well as in antagonistic muscles and the adaption of muscle force to the real loadcase will be performed by passive stretching of the muscles.

The force distribution among different muscles and muscle fibers may also vary in time. If a loading task shall be sustained for a prolonged period of time, one or more muscles may not be able to maintain the force due to fatigue and the force must be taken over by another muscle or other muscles.

Experiments

The literature contains only two experiments performed to validate different optimization cost functions for the trunk system. In both essentially the same models are used.

Schultz et al. (1982b, 1983) compared different optimization cost functions including forces and muscle stress of the system for a great number of different loading tasks and found the best correlation between theoretical muscle force and measured EMG activity for a min-max cost function, namely minimization of the maximum muscle tension. What the min-max cost function actually does is to transform the system to functional muscle units excluding all antagonistic muscle activity. The results from the twist load case, however, were contradictionary to Pope et al. (1985), who found a considerable antagonistic muscle activity in the abdominal wall.

Muscle force distribution assumed

In this work, only mechanical considerations were made. No specific assumption of the muscle control function was made. By means of the functional muscle unit approach the spinal system was reduced to a limit where it was possible to use pure mechanical tools; by making certain assumptions about the distribution of muscle forces (Chapter 6) it was reduced to a statically determinate system. It is difficult to fit these assumptions into any of the three main groups of control sys-

tems discussed, but on the other hand they are not in conflict with any of these systems either. In view of the uncertainty about the appropriateness of specific assumptions several different choices were made. Thus the statically indeterminate systems were treated by presenting different possible solutions. In this way, the mechanical consequences of different assumptions of the muscle force distribution, *i. e.* the control function, can be described.

4. The passive components

Forces from the upper body are transferred from the chest to the pelvis (with the exception of the latissimus dorsi muscles which act from the humerus to the lumbar back), either directly by means of active components - the abdominal pressure and the muscles - or via the spine and further down to the pelvis by means of active as well as passive elements - bone, ligaments etc. Two things are of special interest when discussing the anatomy of the spinal system in connection with the mechanical behavior, namely:

1. Which are the structures involved in the load transfer?
2. What is the magnitude of the stiffnesses of the joints between the skeletal elements?

The second question is raised because the stiffness of the joints of a compressive loaded structure is important in connection with the evaluation of the mechanical stability of the system.

The main components for transfer of the tensile forces are the muscles (Chapter 6).

In this chapter the passive properties of certain parts of the chest, the vertebral column and the pelvis are described.

The thoracic cage

From the spinal point of view, the interesting part of the chest is the connection between the ribs and the thoracic vertebrae and the stiffening influence from the ribs on the spine.

The bony parts of the chest (Sobotta 1968) are the thoracic spine, the ribs and the sternum. The ribs (with the exception of the lower two or three, the floating ribs) are in their forward ends attached by cartilage to the sternum. The unit formed by the bony parts and the cartilage is called the thoracic cage (Figure 4-1). Each of the upper ten ribs articulates with the vertebral column in two places: the head of the rib with two adjacent vertebral bodies and the tubercle of the rib with the transverse process of the lower of the two adjacent vertebrae at the costotransverse articulation (Figure 4-2). The movement of the ribs at the costovertebral articulations and at the costal cartilage is limited by strong ligaments and is best described as a small play (Schultz et al. 1974). The lower two ribs have a single facet on the head and they articulate with the bodies of T11 and T12 respectively. In a muscle relaxed state, the mechanical support from these ribs to the spine probably is small.

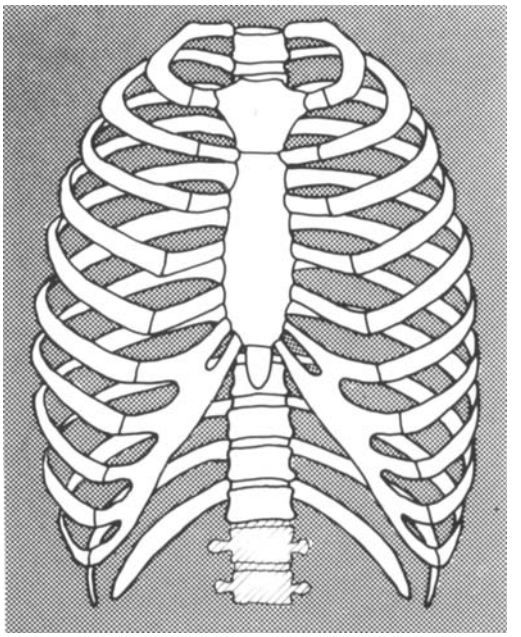

Figure 4-1. The thoracic cage.

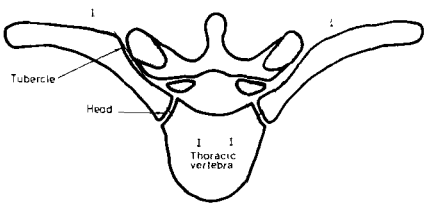

Figure 4-2. The costovertebral articulation. A limited rotation of the ribs is allowed around the axis through the articulations of the head and tubercle of the rib, the I-I axis.

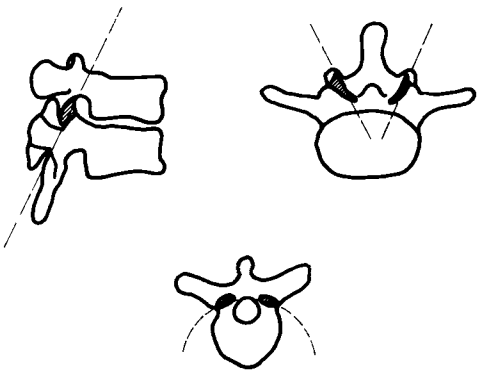

Figure 4-3. The orientation of the articular facets at the thoracic and the lumbar levels. Left and lower: thoracic vertebrae. Right: lumbar vertebra.

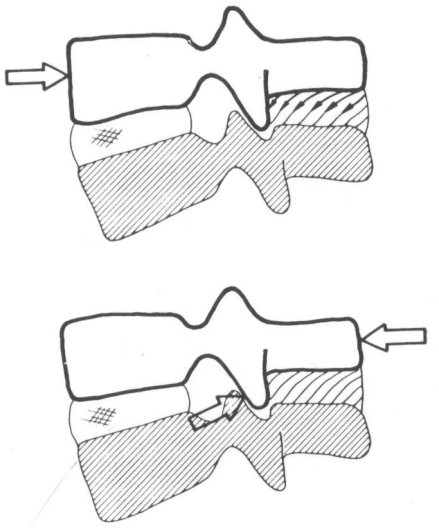

Figure 4-4. Structures counteracting a posterior respectively an anterior shearforce acting on a lumbar motion segment.

Top: force acting in a posterior direction on the upper vertebra is counteracted by passive stretching of the interspinous ligament.

Bottom: force acting in an anterior direction is counteracted by contact forces in facet joints.

The articular facets

The mechanical role of the articular facets is twofold: to give kinematic constraints to the movement of the motion segment and to transfer forces.

The facet joints of two adjacent vertebrae have different geometrical orientation at different spinal levels which influence the kinematic behavior of the spine (White and Panjabi 1978; Figure 4-3).

At the thoracic level, the facets have a basically circumferential orientation and give no rotational restriction on the relative motion of two adjacent vertebrae (rotation is prevented by the ribs in this area).

At the T12-L1 level the orientation of the facets is drastically changed to a basically radial direction which will lock axial rotation. The T12-L1 motion segment has the highest rotatory stiffness of any motion segment (Markolf 1972). Numerical figures for facet joint orientation were presented by Scholten (1986).

In the lower lumbar region, the facet joints are slightly turned into the frontal plane (Taylor and Twomey 1986) so that more axial rotation is allowed and the facet joints are more adapted to withstand the shear force induced due to the forwards slanting orientation of the intervertebral disks at the L4-L5 and L5-S1 levels.

Load transfer between the articular facets of two adjacent vertebrae

The orientation of the articular facets shows that they first of all are intended to transfer a shear force, acting on the upper vertebrae in anterior direction between two adjacent vertebrae. An inspection of the anatomy of the motion segment and results from shear tests presented by Berksson et al. (1979) indicate that a posterior force is counteracted first of all by the interspinous ligament (Figure 4-4).

In flexion, tension forces are also transferred via the capsular ligaments. About 1/4 to 1/3 of the passive flexion stiffness of the motion segment is contributed from stretching of these ligaments (Adams et al. 1980a). For an extended motion segment, compressive forces can be transferred via mechanical contact between the tips of the articular facets and the arc of the vertebra below (Jacob and Suezawa 1985). Adams et al. (1980b), found that in the neutral position, none or only a minor part of the compressive force was transferred by the articular facets.

The motion segments of the ligamentous spine

In order to evaluate the mechanical behavior of the spine, especially for low muscle activity levels, the mechanical characteristics (i.e. the relation between applied load, force or moment, and the corresponding deformation) of the motion segments must be known.

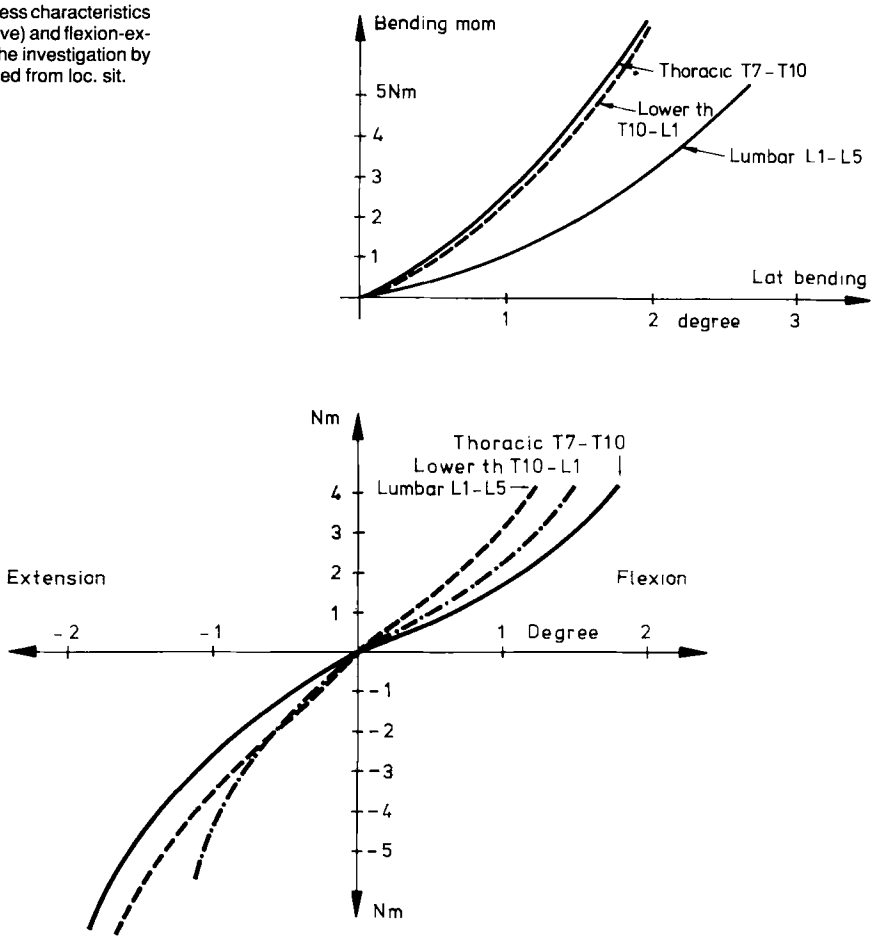

Figure 4-5. The stiffness characteristics in lateral bending (above) and flexion-extension (below) from the investigation by Markolf (1972). Adapted from loc. sit.

The stiffness characteristics are not linear and are more or less dependent of loading in other directions. Thus for example the torsion stiffness has been shown to be strongly dependent on the magnitude of the compressive force (Panjabi et al. 1977).

Of interest when evaluating the mechanical stability and equilibrium in the sagittal and frontal planes of the spine, are the lateral bending, flexion-extension and axial rotation characteristics (Berksson et al. 1979, Lucas and Bresler 1961, Markolf 1972, Nachemsson et al. 1979, Panjabi et al. 1976a, b, Schultz et al. 1979, Skogland and Miller 1980).

The stiffness characteristics at lateral bending and flexion-extension from the investigation by Markolf (1972) are shown in Figure 4-5. The thoracic motion segments were found to be stiffer than those from the lumbar region (Table 1). Interindividual differences in the range -50% to +130% from the mean values were found. No compressive preload was applied during these tests.

Table 1. The mean values of the initial stiffness (i.e. the slope of the torque-rotation curve at zero torque) and the number of motion segments tested (Markolf 1972)

	Motion Segments			
	Thoracic		Lumbar	
	n	Nm/degree	n	Nm/degree
Lateral bending	24	2.0	19	1.3
Extension	19	3.4	15	2.5
Flexion	19	3.0	15	1.8

Evaluation of the influence of axial preload on the bending characteristics must be performed by taking the induced torque from the applied preload into consideration. However, this does not seem to have been considered in previous investigations (Nachemsson et al. 1979, Panjabi et al. 1977a, b, Schultz et al. 1979, Skogland and Miller 1980).

The influence of other loads on the bending characteristics is to my knowledge not presented in the literature.

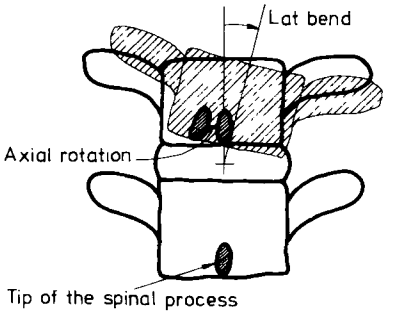

Figure 4-6. The geometrical coupling between lateral bending and axial rotation of a thoracic motion segment.

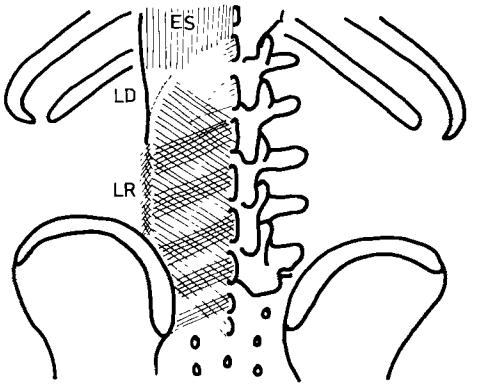

Figure 4-7. The network formed by the superficial and deep laminae of the posterior layer of the thoracolumbar fascia. The two laminae and the middle layer of the fascia are fused at the lateral raphe, LR. ES: the erector spinae and LD: the latissimus dorsi muscles. Adapted from Bogduk and MacIntosh (1984).

The investigation by Adams et al. (1980) shows a shift in the ligamentous structures that resist the flexion moment from the yellow to the capsular ligament. As the capsular ligaments have a more lateral position, this indicates that the lateral bending characteristics depends on the flexion: increased flexion of a motion segment would increase the stiffness.

A theoretical investigation by Broberg (1983), showed considerably increased disk stiffnesses for higher compressive preload in all three rotations, i.e. lateral bending, flexion-extension and axial rotation.

Kinematic coupling between lateral bending and rotation

A geometrical coupling between lateral bending and rotation of two adjacent vertebrae is reported in the literature. The coupling is different for the thoracic and the lumbar regions (White and Panjabi 1978); in the lumbar region, lateral bending is combined with rotation of the spinous processes towards the concave side and in the thoracic region towards the convex side (Figure 4-6) which may be explained by the orientation of the facet joints.

The thoracolumbar fascia

The thoracolumbar fascia consists of three layers: the anterior layer that arises from the anterior surface of the lumbar transverse processes, a middle layer that arises from the tips of the lumbar transverse processes and a posterior layer that arises from the midline and covers the back muscles (Bogduk and MacIntosch 1984).

Considering the anatomy, three different mechanical roles of the thoracolumbar fascia may be distinguished:

1. Force transfer from muscles to skeletal elements.
2. Force transfer directly between sceletal elements (no muscles involved, force is obtained by stretching of the fascia).
3. Transfer of transverse forces between the spine and the erector spinae muscle (retinaculum around the erector spinae muscle).

The superficial lamina of the posterior layer forms the insertion for the latissiumus dorsi to the iliac crest, the sacrum and the spinous processes.

The superficial and deep lamina of the posterior layer together form an oblique network attached to the spinous processes along the midline (Figure 4-7). Cau-

dally this network is attached to the iliac crest and the spinous processes of the sacrum and laterally it is fused to the medial layer of the thoracolumbar fascia at the lateral raphe. In the upper lumbar region, the deep lamina is poorly developed. Here the superficial layer transfers muscle force from the serratus posterior inferior (which probably is not involved in the mechanics of the back) to the spinous processes of the lumbar spine.

Together with the middle layer the network forms a retinaculum which surrounds the erector spinae. As the main direction of the fibers in this retinaculum is transverse to the erector spinae, the thoracolumbar fascia can only to a minor extent be expected to passively resist a flexion moment acting on the trunk.

In Chapter 6, the mechanical role of the the thoracolumbar fascia will be discussed in detail.

The pelvis

The pelvis is the foundation for the lumbar spine. The deformation within the pelvis due to loading from the spine is small and the pelvis will be considered as a rigid body.

5. The local and the global systems

For mechanical modeling of the spinal system, an effective approach has been found by identifying a *local* and a *global* system. The active components (muscles and intraabdominal pressure) involved in transfering forces from the thoracic cage to the pelvis will be assigned either of the systems. Which of the systems an active component will be assigned is judged from a consideration of its main mechanical role — to transfer load directly between the pelvis and the thoracic cage or to act directly on the lumbar spine (between the vertebrae or from the lumbar spine to either the pelvis or the thoracic cage).

The main role of the global system appears to be to balance the outer load so that the resulting force transfered to the lumbar spine can be handled by the local system. Thus large variations of the distribution of the outer load should give rise to only small variations of the resulting load on the lumbar spine. The local system, therefore, is essentially dependent on the magnitude (not the distribution) of the outer load and of the posture (curvature) of the lumbar spine.

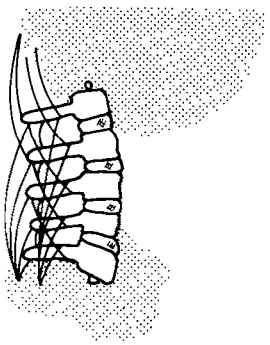

Figure 5-1. The local system is formed by the muscles attached to the lumbar vertebrae.

The local system

All muscles which have their origin or insertion at the vertebrae, with the exception of the psoas, are defined as belonging to the local system (Figure 5-1).

The local system is used to control the curvature and to give sagittal and lateral stiffness to maintain mechanical stability of the lumbar spine.

The psoas muscle is not included in the local system as its mechanical role obviously is global (flexor of the hip joints).

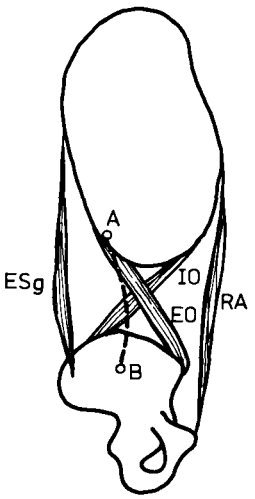

Figure 5-2. The global system is formed by the muscles and the intra-abdominal pressure, i.e the active components which transfer load directly between the thoracic cage and the pelvis. The muscles schematically shown are: ES: global erector spinae muscles, IO: internal oblique, EO: external oblique and RA: rectus abdominal muscles. Not shown are the intra-abdominal pressure and the global part of the quadratus lumborum muscle. AB: the lumbar spine (not included in the global system).

The global system

The global system consists of the active components, *i.e.* the muscles and the intra-abdominal pressure, which transfer the load directly between the thoracic cage and the pelvis (Figure 5-2). The muscles included are: the global erector spinae muscles, the internal and external obliques, the rectus abdominal muscles and the lateral parts of the quadratus lumborum muscles

(inserted at the twelfth ribs). In addition the psoas should be referred to the global system. The latissimus dorsi muscles, which act from the lumbar back to the humerus, primarily transfer load from the humerus to the pelvis. Indirectly these muscles may influence the stability conditions for the lumbar back. It is however judged that the psoas muscles and the latissimus dorsi muscles do not have a substantial role in maintaining mechanical stability of the back system. It can even be stated that stability of the spinal system must be maintained in spite of action in these two muscle groups. The psoas and the latissimus dorsi muscles were therefore excluded from the analysis.

The line of action of the force from the global system, which will be counteracted by the local system, must always pass forward of or through the midpoint of the most anterior lumbar disk. Otherwise this force would extend the lumbar spine with no possibility for the muscles of the local system to reinforce it without causing further extension. In other words: equilibrium could not be satisfied (with given curvature of the lumbar spine).

The global system can be said to respond to changes of the line of action of the outer load, whereas the local system responds to changes of the posture of the lumbar spine. Both systems respond to changes of the magnitude of the outer load. Naturally, the global system also is used to change the position of the thoracic cage cage in relation to the pelvis.

There is one ambiguity in the distinction between the local and the global systems concerning the muscle attached to the erector spinae aponeurosis, ESA. This aponeurosis is the origin for the global erector spinae muscle and it arises from the dorsal segment of the iliac crest, the sacral and lumbar spinous processes and the intervening supraspinous ligaments. According to the definition, those muscle fibers which use the parts of the ESA which are attached to the lumbar spinous processes and the intervening supraspinous ligaments would belong to the local system. The main mechanical role of the ESA is however to transfer tensile forces in the global erector spinae muscle to the pelvis, i.e. the role of the global system. Accordingly all parts of the erector spinae thoracic fibers are assigned the global system (the global erector spinae muscle).

The intra-abdominal pressure theoretically has a global and a local mechanical role. The global role is to act directly on the thoracic cage or on the curved global muscles. The local action consists of the transverse force in the posterior direction acting directly on the lumbar spine thus, inducing a flexion moment.

The muscles between the lumbar vertebrae

Throughout the spine (in the cervical, thoracic and lumbar regions) there are *multifidi* muscles attached to the vertebrae. The lumbar multifidi muscle fibers have their insertions on the spinous processes and their origins on the mammilar processes two or more vertebrae below (Figure 5-3).

The *interspinal* and the *intertransverse* muscles act between two adjacent vertebrae with their insertion and origin on the spinous respectively the transverse processes (Figure 5-4).

Considering the great differences in the areas of the muscles (which imply great differences in maximum

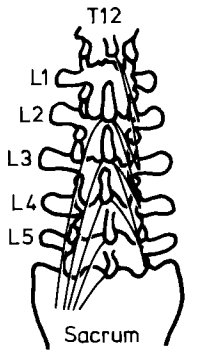

Figure 5-3. The multifidi muscles of the lumbar back. The muscle fibers between the vertebrae and the pelvis are shown to the left and some of the muscle fibers between the vertebrae to the right.

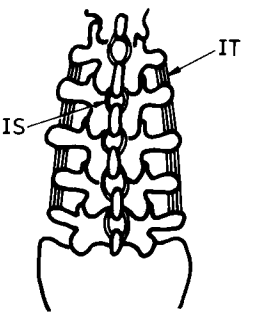

Figure 5-4. The interspinal and the intertransverse muscles of the lumbar back.

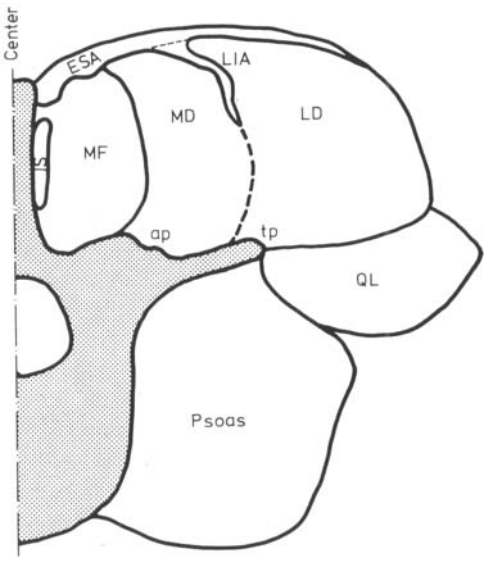

Figure 5-5. Cross-section through L4. LD: Erector spinae, lateral division, MD: Erector spinae: medial division, MF: multifidi, IS: interspinalis, QL: quadratus lumborum muscles, LIA: lumbar intermuscular aponeurosis, ESA: erector spinae aponeurosis, ap: accessory process and tp: transverse process. The interspinalis muscle is normally not seen on a cross-cut through a lumbar spinous process. It is placed in this figure only to show its relative muscle area. The medial and lateral divisions of the erector spinae muscle contains fibers inserted to the accessory and outermost tip of the transverse processes respectively. Adapted from Bogduk (1980) and from the cross-cut photographs from the investigation by Jonsson (1970).

muscle forces) and the differences in muscle lengths, different mechanical roles of the muscles can be identified. The stiffness of a muscle is approximately proportional to the muscle force and inversely proportional to the muscle length, see further Chapter 6 and Bergmark (Appendix 2, 1987).

The multifidi muscle areas found by Langenberg (1970) for two young male spines were about 2x3.5 cm^2 in the upper lumbar region and 2x6 cm^2 in the lower lumbar region (Figure 5-5). The muscle area of the interspinal muscles is less than 2x1 cm^2 according to the cross-cut photographs from the investigation by Jonsson (1970). The transverse area of the intertransverse muscles is hard to determine from the cross-cut photographs but can be assumed to be of the same order as the area of the interspinal muscles.

The mechanical role of the multifidi muscles therefore is more emphasized on transfer of forces and to act as a mover, thus controling the lordosis, while the intertransverse and the interspinal muscles will, in spite of their comparatively small muscle force but due to their short length, give an increased stiffness and thus extrinsic mechanical stability to the spine.

The muscles from pelvis to the lumbar vertebrae

The *multifidi* fibers between the lumbar vertebrae and the pelvis, originate from the sacrum and the iliac crest and are inserted to the spinous processes.

The medial and lateral divisions of the *erector spinae* muscle (Figure 5-5) both have lumbar as well as thoracic fibers. The thoracic part, which is about 2/3 of the muscle area (Bogduk 1980), belongs to the global system and the remaining 1/3, the lumbar part, belongs to the local system. The anatomy of the lumbar muscles is very carefully described by Bogduk (1980). The lumbar fibers of the medial division originate from the medial part of the iliac crest and the lumbar intermuscular aponeurosis (LIA), and are inserted into the accessory processes of the lumbar vertebrae. The major part of the lumbar fibers of the lateral division originates from the ilium and a minor part from the LIA. They are inserted into the outermost parts of the transverse processes of the lumbar vertebrae. The lumbar part of the erector spinae muscle with insertions to the lumbar vertebrae will in the following be called "local erector spinae muscle fibers".

The *quadratus lumborum* originates from the iliac crest and inserts at the outermost part of the transverse processes of the lumbar vertebrae. The lateral part of this muscle inserts at the lowest floating rib and therefore belongs to the global system.

The insertions into the lumbar vertebrae of the local part of the erector spinae and the quadratus lumborum muscles are shown in Figure 5-6.

Consideration of the insertions to the vertebrae indicates the mechanical roles of the different muscles. The multifidi muscles extend the lumbar spine. As they insert at the spinous processes and the fibers are essentially parallel to the vertebral column, there is only a minor influence in the lateral direction.

The lumbar erector spinae muscle fibers also extend the spine, but in a less efficient way because of the shorter sagittal lever arms compared to the multifidi muscles. Unilateral activity gives the combined mechanical function of extension and lateral bending of the lumbar spine. Bilateral action extends the lumbar spine and stabilizes the spine mainly in the lateral direction.

The local part of the quadratus lumborum muscles stabilizes the spine in the lateral direction. Unilateral action induces lateral bending of the lumbar spine.

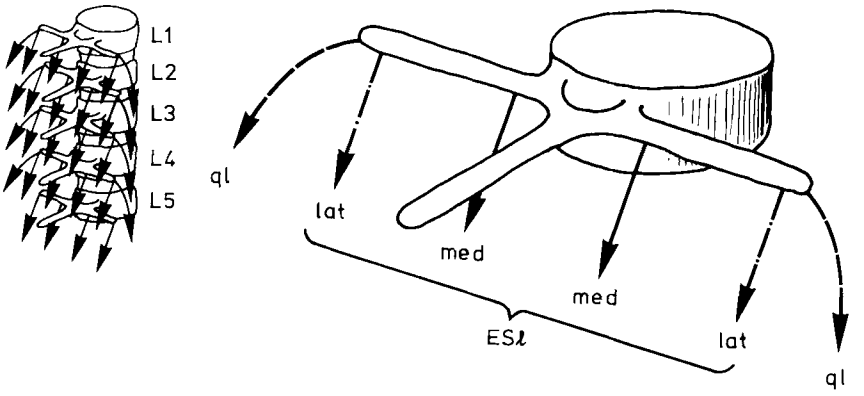

Figure 5-6. Insertions of the local erector spinae and quadratus lumborum muscle fibers to the lumbar vertebrae. The origins are at the pelvis. ql: quadratus lumborum fibers inserted to the outermost part of the transverse processes of L1 to L4. ESl: local erector spinae muscle fibers. med: medial fibers of ESl inserted to the accessory processes of L1 to L5 and lat: lateral fibers of ESl inserted to the outermost part of the transverse processes of L1 to L5.

The mechanical role of the global part of the quadratus lumborum muscles, which act between the pelvis and the twelfth ribs, is to counteract activity in the diaphragm.

The muscles from the thoracic cage to the lumbar vertebrae

The *multifidi* muscle bridge the T12-L1 level; they originate from the mammilar processes of the lumbar vertebrae and they insert at the spinous processes of the thoracic vertebrae.

The *spinalis* muscle originates on the spinous process of the upper lumbar and lower thoracic vertebrae. Different information about the lower level of attachment, T12 (Sobotta 1968) or L1 (Langenberg 1970) is given in the literature. The insertion is to the spinous processes of the upper thoracic vertebrae. These muscles extend the upper lumbar and the thoracic spine.

The muscles from the thoracic cage to the pelvis

The thoracic fibers of the *erector spinae* muscle originate from the erector spinae aponeurosis (ESA). The fibers of the medial division (Figure 5-5) originate from the deep (anterior) surface of the ESA and are insert at the transverse processes of the thoracic vertebrae and the ribs. The muscle fibers are essentially parallel to the spine. The fibers of the lateral division originate from the posterior surface and the upper end of the ESA and insert at the ribs. The most lateral part of the fibers of the lateral division have an oblique caudal-medial direction.

The mechanical role of the global erector spinae muscles is to extend the trunk and stabilize the spinal system in the sagittal and lateral directions. Unilateral activity will induce lateral bending and extension of the thoracic cage.

The *external oblique* abdominal muscle originates from the lower eight ribs. It inserts at the cartilage of the lower three or four ribs and by aponeurosis at the cartilage of the seventh to ninth ribs and to the rectus sheath (Sobotta 1968). The dorsal border is free. The mechanical role obviously is global: bilateral action in the upper part induces flexion and unilateral action flexion- rotation of the thoracic cage.

The *internal oblique* abdominal muscle originates at the lateral raphe of the thoracolumbar fascia (Bogduk and MacIntosch 1984), the iliac crest and the inguinal ligament. It is inserted at the costal cartilage to the midline by direct attachment to the cartilage of the lower two or three (false) ribs and via the internal oblique aponeurosis to the rectus sheath (Sobotta 1968).

The main mechanical role of this muscle is global: bilateral action induces flexion and unilateral action flexion–lateral bending of the thoracic cage.

The mechanical roles of the oblique muscles in combination with loading in axial rotation does not, however, seem to be simple. An experimental study by Pope et al. (1985) of muscle activity patterns in the oblique muscles during twist loading from an outer force couple, showed no essential difference in activity in left and right internal obliques and of activity in left and right external obliques.

In addition to the global action of the internal oblique also a minor lateral local action on the lumbar vertebrae via the lateral raphe and parts of the thoracolumbar fascia is possible.

The external and the internal oblique abdominal muscles are both curved. Force transfer in these muscles therefore must be associated with an intra-abdominal pressure.

The intra-abdominal pressure

The abdominal cavity contains mainly liquid and viscous material and may be considered as a non-compressible fluid. The intra-abdominal pressure is maintained by activity in the surrounding muscles, anteriorly by the rectus abdominis, laterally by the external and internal oblique abdominal muscles and the transversus abdominis, above by the diaphragm and below by the muscles of the pelvis floor. Probably, only one of the three lateral abdominal wall muscles, *i. e.* the external or the internal oblique or the transversus muscles is needed to maintain the intra-abdominal pressure. This liberty of choice opens the possibility for the intra-abdominal pressure to be maintained with or without tensile forces acting between the thoracic cage and the pelvis in the abdominal wall.

As these three muscles are curved, the contrary is also valid: activity in either of them provokes intra-abdominal pressure (Broberg 1981).

The mechanical role of the intra-abdominal pressure is not completely understood and is still a question focused by biomechanical researchers.

In vivo experiments show a strong positive correlation between increased loading on the trunk and the magnitude of the intra-abdominal pressure (Grew 1980, Hemborg 1983).

Theoretically at flexion and extension loading of the thoracic cage, the global action of the intra-abdominal pressure may decrease the compressive load acting in the spine about 15-30% (Broberg 1981)

In vivo experiments, however, showed that the Valsalva maneuver did raise the intra-abdominal pressure, but it increased rather than decreased the L3-L4 disk pressure and thus also the lumbar spine compression (Nachemsson et al. 1986).

The intra-abdominal pressure is also capable of flexing the lumbar spine by direct local action on the vertebrae. This opens the possibility for increased muscle reinforcement from sagittal local muscle action (multifidi and interspinal muscles) without changing the equilibrium conditions for the system as a whole.

6. Mechanical stability of the lumbar spine

How *stable equilibrium* is maintained in the spinal system constitutes a central issue of the present work. It is therefore important to clarify what this concept actually stands for. To this end a mechanical system far simpler than the spinal system will be discussed. Two versions, A and B, of this system are shown in Figure 6-1; Equilibrium with the standing T can be obtained in both versions. It is simply a matter of adjusting the screw until the force in the spring equals the weight Q. The spring in system B must be stretched much more than the spring in system A as a consequence of the difference in spring stiffness. However, this equilibrium is *stable* only if the spring is stiff enough. *Thus the A version may represent a stable and system B an unstable equilibrium.*

To check whether an equilibrium state is stable or not, an arbitrarily small disturbance should be assumed. In practical applications disturbances are inevitable. Assume that the disturbance consists of a small clockwise angular deviation, $\Delta\varphi$, from the upright position of the T, (Figure 6-2). The force Q tries to increase the disturbance angle $\Delta\varphi$, whereas the force P in the spring tries to move the system back to the equilibrium position $\Delta\varphi = 0$. Thus the question about stability and instability is reduced to the question about which one, P or Q, that wins.

Since the spring has been elongated, the force P is larger than Q, the equilibrium value. Can this compensate for the decreased lever arm for P (with respect to rotations around the hinge) and the increased lever arm for the weight Q? Obviously the same $\Delta\varphi$ implies a larger increase of P the stiffer the spring is. Therefore one arrives at the conclusion that stable equilibrium prevails if the spring is stiff and that the equilibrium is unstable if it is not. The same conclusion is arrived at in a similar way for an anti-clockwise angular deviation $\Delta\varphi$ instead of the clockwise one shown in Figure 6-2. Some critical stiffness exists above which the equilibrium is stable and below which it is unstable.

The problem now consists of how to calculate the critical stiffness. Fortunately powerful methods exist by means of which this problem can be solved, even for much more complicated systems than the one just treated. Moreover the underlying basis is simple: *Stable equilibrium prevails when the potential energy of the system is minimum.*

In the example shown in Figure 6-2, the potential energy consists of two components. One is the potential

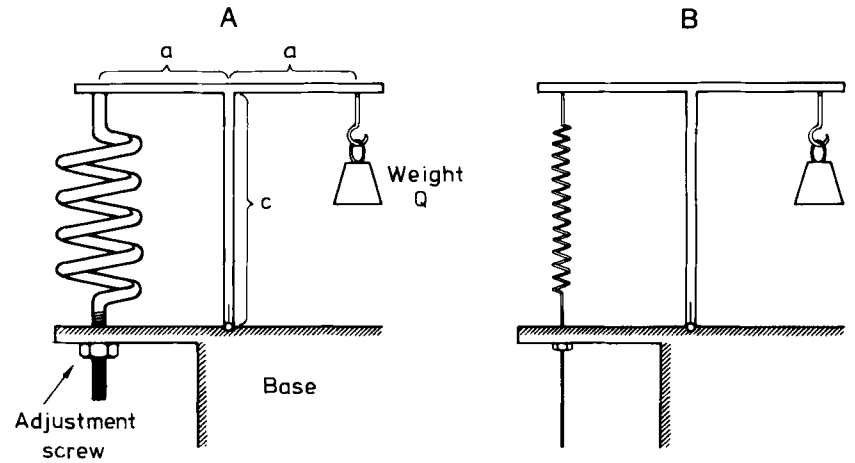

Figure 6-1. The two versions of the system for illustration of the concept of mechanical stability. System A has a much stiffer spring than system B. The lateral stiffness of the springs is assumed to be small enough to be neglected.

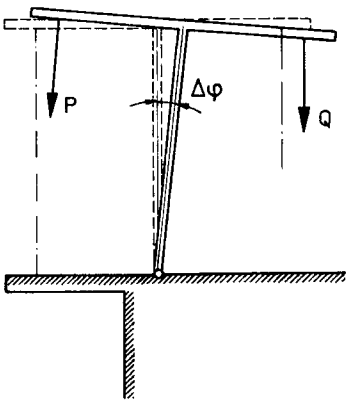

Figure 6-2. The system opposed to an angular small disturbance $\Delta\varphi$.

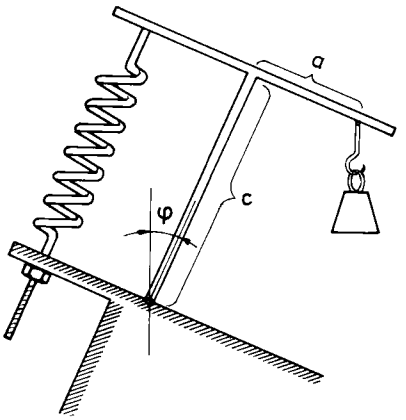

Figure 6-3. By appropriate adjustment of the tension of the spring, equilibrium can be obtained for an inclined position of the system. φ is the inclination of the T.

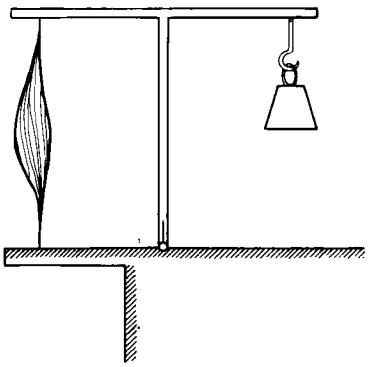

Figure 6-4. The system considered when the spring is exchanged by a muscle.

energy of the weight Q. This decreases the amount $Q \cdot \Delta$ when the weight moves the distance Δ towards a lower level. The other component is the energy stored in the spring. It increases by the amount $Q\delta + 1/2 \cdot k\delta^2$ when the spring is elongated a small distance δ from its equilibrium position. k is the spring stiffness. The potential energy (Bergmark 1987, Appendix 3) of the system shown in Figure 6-2 has a minimum for $\Delta\varphi = 0$ if the spring stiffness $k > k_{crit}$ where

$$k_{crit} = Q\, c/a^2 \qquad (6.1)$$

Equilibrium can be obtained also for other positions of the T than the upright one (Figure 6-3). Again a critical stiffness exists, above which the equilibrium is stable and below which it is unstable.

Now, assume that the spring in the simple system regarded is exchanged for a muscle (Figure 6-4). There is no need for an adjustment screw, because within certain limits a muscle has the ability to furnish any desired force at fixed length.

A disturbance $\Delta\varphi$ could now, in principle, be met in two different ways. One is operative when the muscle stiffness is high enough. Stability is then automatically maintained as soon as equilibrium is reached. In the other way, necessary when the muscle stiffness is too low, equilibrium is lost as the system is mechanically unstable but the deviation from the upright position is kept small by continuous and appropriate adjustment of the muscle force beyond simple stiffness control.

In the first case, the muscle force is changed by passive stretching of the filaments and by spinal reflex adjustment of the tension. In the second case, supra spinal control is needed.

Muscle stiffness

The stable equilibrium can be maintained if the muscle stiffness (which is constituted by passive stretching and spinal reflex tension modification) is greater than the critical stiffness according to expression (6.1). The relation shows that the minimum passive stiffness required must be higher the higher the muscle force is. This, incidentally, seems to be precisely the case (Morgan 1977, Rack et al. 1974). Note that, on the contrary, the stiffness of an ordinary mechanical spring, like a helical spring, is nearly independent of the spring force. Moreover, the muscle stiffness for a small elongation, to a first approximation seems to be proportional to the current muscle force (Morgan 1977). Therefore one can write:

$$k = q\, F/L \qquad (6.2)$$

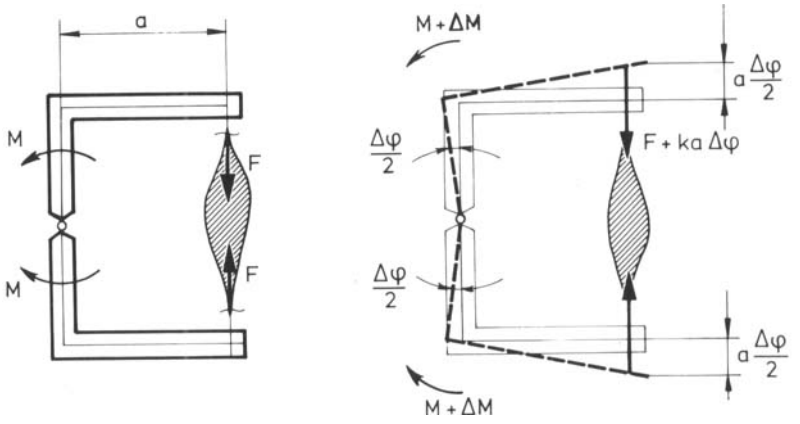

Figure 6-5. To the left: A skeletal joint is subjected to an outer torque M. Equilibrium is maintained at the given position by action of the bridging muscle.

To the right: Due to the action of a small additional torque ΔM, the two elements will rotate a small angle Δφ relative to each other. k is the muscle stiffness defined in (6.2).

where k is the muscle stiffness, q a numerical factor, the *muscle stiffness coefficient*, F the muscle force and L the muscle length. It is assumed that q is the same for all skeletal muscles. The magnitude of q seems to be around 40 (Bergmark 1987, Appendix 2).

Torque stiffness of a joint

It is here convenient also to define the *torque stiffness*, λ, of a joint with one or more bridging muscles.

First, assume that the joint (Figure 6-5), is frictionless and that the passive stiffness of the muscles and other bridging tissues (mainly ligaments) can be neglected. Equilibrium is maintained at the given position by appropriate action of the muscle:

$$M = Fa \qquad (6.3)$$

where M is the outer moment, F is the muscle force and a is the muscle lever arm.

If the torque is suddenly increased an amount ΔM, the two skeletal elements will rotate an angle $\Delta\varphi$ relative to each other. It is assumed that $\Delta\varphi$ is small, *i.e.* $|\Delta\varphi| \ll 1$.

The torque stiffness is defined as:

$$\lambda = \Delta M/\Delta\varphi \qquad (6.4)$$

After some elaborations (Bergmark 1987, Appendix 3) one obtains the torque stiffness:

$$\lambda = q\,Fa^2/L \qquad (6.5)$$

It is thus possible to use either of two ways to describe the stiffening influence from the single joint muscles: either the direct muscle stiffness according to (6.2) or the torque joint stiffness according to (6.5).

Now consider also the (passive) stiffness λ_o of the joint itself, *i.e.* the joint is still frictionless but the elastic properties of the bridging passive tissues (mainly ligaments) will be regarded. This gives rise to a moment M_o in the equilibrium position. M_o depends on the position (relative rotation of two elements) and there exists one "neutral" position at which $M_o = 0$. The passive torque stiffness, λ_o, of the joint is in this case added to the stiffness contribution from the muscles:

$$\lambda = \lambda_o + q\,Fa^2/L \qquad (6.6)$$

In the case of a bilateral stabilized joint synergistic and antagonistic muscle action might be present independent of the outer torque acting over the joint. For a symmetric and symmetrically loaded bilateral joint, the torque stiffness is

$$\lambda = \lambda_o + q\,2Pa^2/L \qquad (6.7)$$

where P is the muscle force in each side.

As an example of a stability discussion using the concept of torque stiffness, the ankle joint will now be considered.

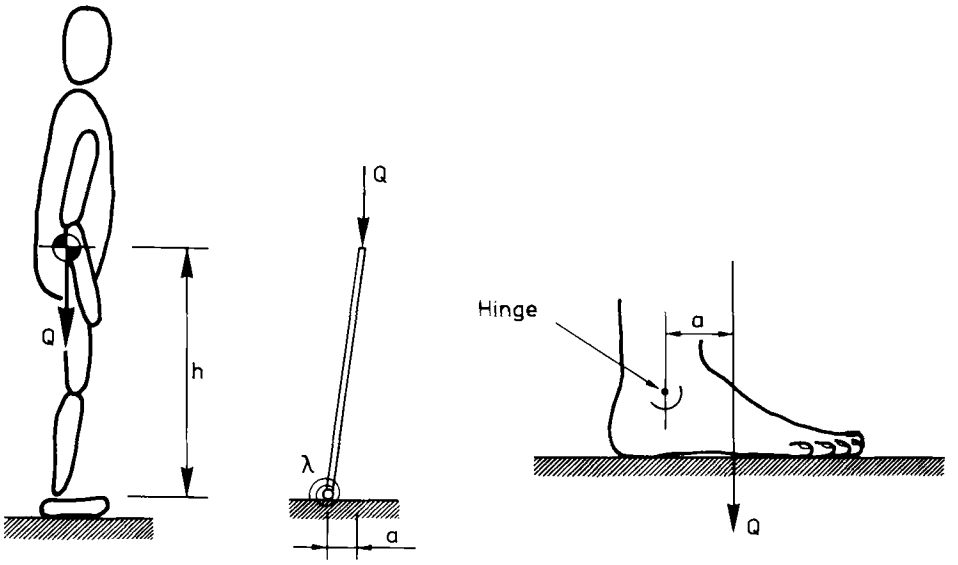

Figure 6-6. The body considered as a rigid inverted pendulum. Q: gravity force, a: distance from the hinge to gravity line, h: vertical height to the center of gravity of the body and λ: torque stiffness of the ankle joint.

The ankle joint stability

An estimation of the sagittal stability of the ankle joint can be made by considering the body as a rigid inverted pendulum (Figure 6-6).

It is here convenient to use the torque joint stiffness formulation of the muscle stiffening influence.

The critical joint torque stiffness for mechanical stability of the inverted pendulum is (Bergmark 1987):

$$\lambda_{crit} = Qh \qquad (6.8)$$

where Q is the vertical load per ankle joint (in this case half the body weight above the feet) and h the height at which Q is applied (Figure 6-6).

Data on the ankle joint stiffness are presented (Hunter and Kearney 1982, 1983) and (Kearney and Hunter 1982). According to their experiments, the ankle stiffness is dependent on the mean ankle torque carried by the ankle and the displacement (rotation) amplitude. The mean stiffness value for plantarflexion obtained in their investigation (see also Figure 6-7) is:

$$\lambda \approx \lambda_0 + \kappa M \qquad (6.9)$$

At about 5 degrees peak to peak value they found $\lambda_0 =$ 35 Nm/rad, $\kappa = 12.4$ rad^{-1}. M is the torque carried by the ankle joint.

At about 2.3 degrees peak to peak displacement, the stiffness was found to be about 15 % higher (Kearney and Hunter 1982).

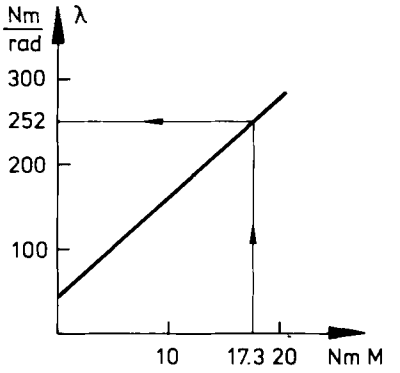

Figure 6-7. Ankle stiffness in plantarflexion, *i.e.* activity in the gastrocnemius-soleus muscles (Hunter and Kearney 1982).

Data for the standing posture are presented by Bendix et al. (1984). In an investigation on 18 women, they found that the gravity line passed on the average a = 63 mm anterior to the lateral malleolus. The mean height of the subjects was 166 cm and the mean weight 55.7 kg (2Q ≈ 550 N).

According to (6.8) and using h = 0.9 m, the critical ankle joint stiffness needed for mechanical stability is $\lambda_{crit} \approx 1/2 \cdot 550 \cdot 0.90$ Nm/rad = 248 Nm/rad (The weight above the ankle joint is approximately taken as the whole body weight). The actual stiffness, λ, must be larger than this value. The results by Bendix et al. together with (6.9) enable calculation of λ.

The torque in (6.9) is found to be:

$$M = Qa \approx 0.5 \cdot 500 \cdot 0.063 \text{ Nm} \approx 17.3 \text{ Nm} \qquad (6.10)$$

From (6.9) one then obtains $\lambda = (35 + 12.4 \cdot 17.3)$ Nm/rad ≈ 252 Nm/rad for plantarflexion at 5 degrees peak to peak rotation and $\lambda \approx 1.15 \cdot 252$ Nm/rad ≈ 290 Nm/rad at 2.3 degrees. Thus $\lambda > \lambda_{crit}$ in both cases. However, the closeness between λ and λ_{crit} is conspicuous. One wonders if it is an coincidence.

There are two facts which indicate that the closeness of the results is based on a rational behavior of the muscle control system.

First, the stiffness of the ankle joint is depending on the moment carried by the joint. By leaning more or less forward, the moment carried by the muscles attached to the achilles tendon changes and thus the stiffness. There is definitely a possibility for the body to "choose" a proper stiffness by adjusting the posture.

Secondly, to maintain mechanical stability, it is sufficient that the ankle joint stiffness exceeds the critical value. A substantially higher stiffness would demand more, unnecessary, muscle activity and thus more energy would be consumed.

Actually, as remarked in Introduction, the stiffness can be somewhat, but not much, lower than the critical value since this implies such a slow magnification of a disturbance that there will be ample time for the nervous system to arrange necessary corrections.

One may conclude that the posture control system appears to be capable of controlling the muscle activity in an optimal way.

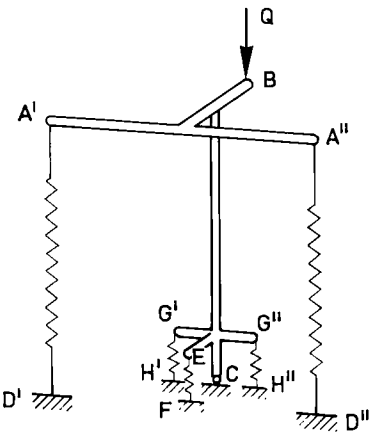

Figure 6-8. Simple example for demonstration of the method for evaluation of the stability of a system containing a global and a local system. A'A"B corresponds to the thoracic cage and G'G"C corresponds to the lumbar spine with a joint at C. A'D' respectively A"D" correspond to the global erector spinae muscle and G'H', G"H" and EF correspond to the local muscles.

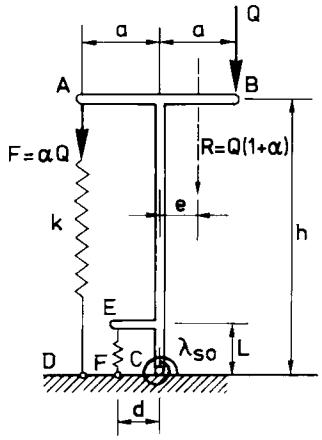

Figure 6-9. Sagittal projection of the system in Figure 6-8. The model is used for the study of the sagittal stability of the simple system.

The spinal system — general considerations

The analysis of the mechanical conditions for stability of the lumbar spine will follow the outline of the examples already discussed.

The stiffness of the back system is depending on the forces in the back muscles. These in turn are depending on the posture and the load. In this way a relation between *load-posture* and *stability* will be found.

Simple example

So far, onedimensional models (*i. e.* rotation around the hinge in the sagittal plane) are considered only. For demonstration of the method used for evaluation of the mechanical stability of the back, the load-posture stability conditions for the simple system shown in Figure 6-8 will be shown. The system can be considered as an extremely simple model of the lumbar spine. The hinge is change to a three-dimensional joint corresponding to the behavior of a motion segment of the lumbar spine. Flexion-extension, lateral bending and axial rotation is allowed at the joint. The purpose with this demonstration is to show how the stability conditions are quantified and also to show the influence on

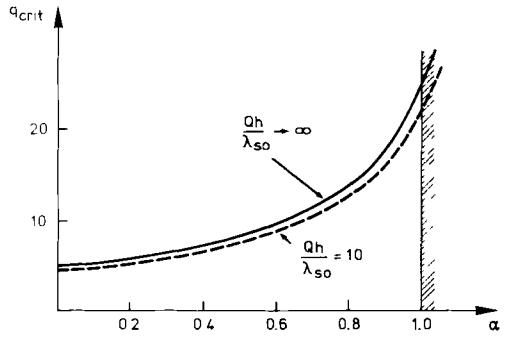

Figure 6-10. Sagittal stability diagram of the system in Figure 6-8. λ_{so} : passive sagittal torque stiffness. Stability requires that the muscle stiffness coefficient $q > q_{crit}$. Regardless of q, equilibrium cannot be satisfied if $\alpha > \alpha_c = 1$.

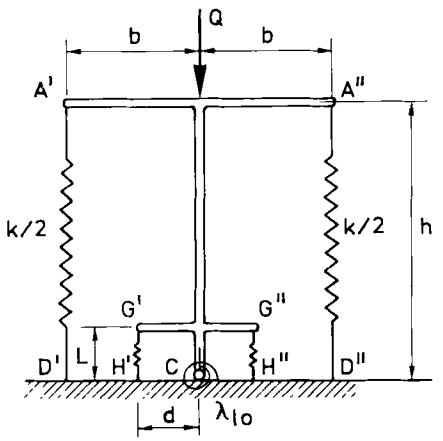

Figure 6-11. Frontal projection of the system in Figure 6-8.

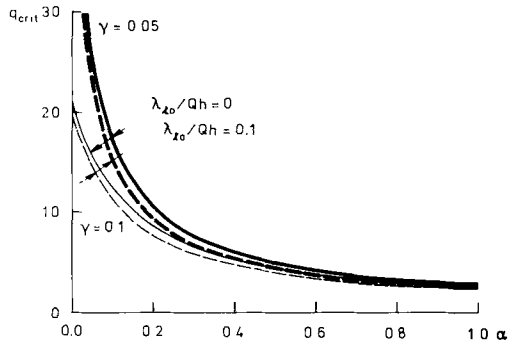

Figure 6-12. Lateral stability diagram for the system shown in Figure 6-8 and 6-11 for two different values of the force in the local lateral muscles, γ = 0.05 and 0.1, and for two values of the passive lateral stiffness of the hinge, $\lambda_{lo}/Qh = 0$ and 0.1. The geometrical properties of the system are h/b = 5/3, h/L = 5 and d/b = 1/2. Stability requires that the the muscle stiffness $q > q_{crit}$.

the stability conditions when muscle activity is moved from the local to the global system.

Symmetric loading is considered all the time. This implies that the muscle activity always must be symmetric (the muscle forces in A'D" and A"D" respectively G'H' and G"H" are always equal).

Sagittal stability

Equilibrium of the simple system in the sagittal plane can be maintained for any global muscle force F in the range $0 \leq F \leq Q$ (Figure 6-9). With the notation $F = \alpha Q$ the condition is $0 \leq \alpha \leq \alpha_{crit}$ where α_{crit} is the upper limit for α. In this case $\alpha_{crit} = 1$. For $\alpha = 0$, the moment from the outer load Q, is counteracted by the muscle activity in the local system only, *i.e.* the muscle force in EF. When α is increased from 0 to 1 the counteracting role is succesively taken over by the global system.

Sagittal stability for the system is maintained when the total sagittal torque stiffness λ_s at the joint C, constituted by the passive torque stiffness in flexion-extension and the local and global systems, is greater than the critical value λ_{crit}. The torque stiffness is in turn depending on the muscle forces, the geometry and the muscle stiffness coefficient as defined earlier (page 27). For a specified geometry and muscle force distribution defined by α, the stability condition can be expressed as a necessary value for the muscle stiffness coefficient, in the following called q_{crit}.

One example is shown in Figure 6-10. From the diagram, one observes that the local system for the given geometry has a more efficient sagittal stabilizing influence compared to the global system.

Lateral stability

The lateral stability conditions are obtained from an analysis of the system shown in Figure 6-11. The condition for equilibrium demands symmetric muscle activity. The muscle forces in the global system are given from the condition for sagittal equilibrium as described in the previous section.

The geometry of the simple model is chosen so the muscle activity in the local sagittal system has no influence neither on the lateral equilibrium nor on the lateral stability. There are no restrictions on the tensile forces in the local lateral system, i.e. the G'H' and G"H" muscle fibers, other than that they must have the same magnitude. For the symmetric loadcase considered here, the only mechanical role of the local lateral system therefore is to stabilize the joint. The force at each

side of the local system is defined by γ: $F_{G'H'} = F_{G''H''} = \gamma \cdot Q$.

Two parameters (α and γ) are necessary to completely define the muscle forces. In Figure 6-12, the lateral stability diagram is shown for a few choices of local lateral muscle activity.

The complete stability diagram

When sagittal and lateral stability are considered, the complete stability diagram shown in Figure 6-13 is obtained. One observes that stable equilibrium is maintained for a range of α provided that the muscle stiffness coefficient q is high enough. The diagram has three limits: one from the lateral stability, one from the sagittal stability and one limit concerning the possibility to maintain sagittal equilibrium.

The same type of diagrams will now be presented for the real back system. For the quantitative analysis of the real spinal system, however, a much more complex model compared to the simple systems considered so far is needed.

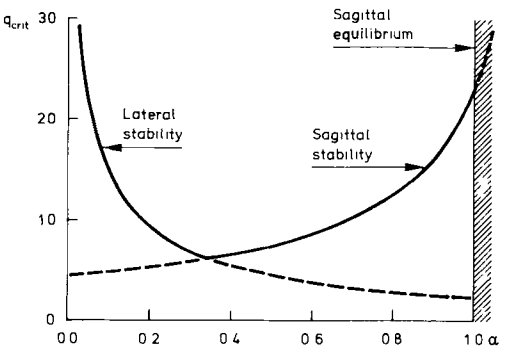

Figure 6-13. The complete stability diagram for the system shown in Figure 6-8. $\lambda_{so}/Qh = 0.1$, $\lambda_{lo}/Qh = 0.1$ and $\gamma = 0.1$. q_{crit} is given by the full-drawn line. Stability requires that the muscle stiffness coefficient $q > q_{crit}$. Regardless of q, equilibrium cannot be satisfied for $\alpha > \alpha_c = 1$.

Realistic model

For the analysis of the real system a three-dimensional model is created (Figure 6-14).

In this investigation, the interest is focused on the lumbar spine. It is assumed that the thoracic cage, including all thoracic vertebrae, is much stiffer than the lumbar spine. Therefore the thoracic cage is considered as a rigid body. The lumbar spine is modeled as 5 jointed rigid vertebrae and the pelvis is the rigid base. The joints at which the rigid skeletal elements are connected to each other are assumed to be placed at the midpoints of the disks.

Since the projection of the spinal system is essentially straight in the frontal plane and S-curved in the sagittal plane the model is given the same features. Its geometrical properties are specified in the next section.

In cases when an outer load is included this is assumed to be realized by a weight carried on the shoulders.

Here only postures and loadings which are symmetric with respect to the sagittal plane will be considered. The deformation mode at mechanical instability is, however, not necessarily symmetric. Therefore the model must be given enough freedom to deform. Thus an individual vertebra must be allowed to rotate around all three axes, i.e. each vertebra is given three degrees of freedom, the rotations $\Delta\varphi_x$, $\Delta\varphi_y$ and $\Delta\varphi_z$. Because of this, any instability mode may occur: pure sagittal,

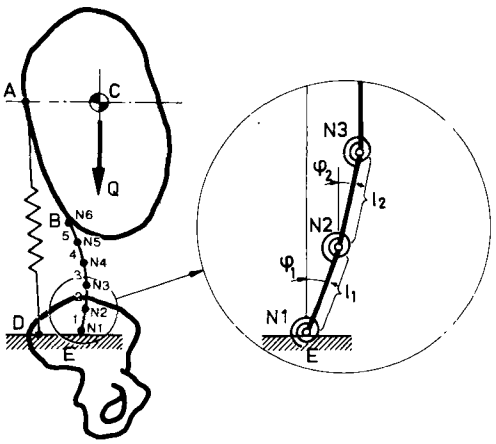

Figure 6-14. Sagittal projection of the realistic model for evaluation of the mechanical stability of the spinal system. ABC: the stiff thoracic cage, DE: the pelvis, BE: the lumbar spine. The rigid vertebrae are interconnected by the torque springs N1,...,N6 (illustrated by filled circles to the left). The numbering of elements, nodes etc of the model always starts from the pelvis. L5 corresponds to element number 1 and N1 is the L5-S1 interconnection. AD: the global erector spinae muscle and C: the center of gravity of the upper body. l_i and φ_i are the length and the inclination of each element. The local muscles shown in Figure 6-15 are also included in the model.

lateral or rotational modes or a combination of these.

Since the intervertebral disks are comparatively stiff with respect to axial and shear deformations, it is assumed that disturbances of this kind can be neglected.

In addition to the global erector spinae muscle pair, muscle fibers corresponding to four local muscle

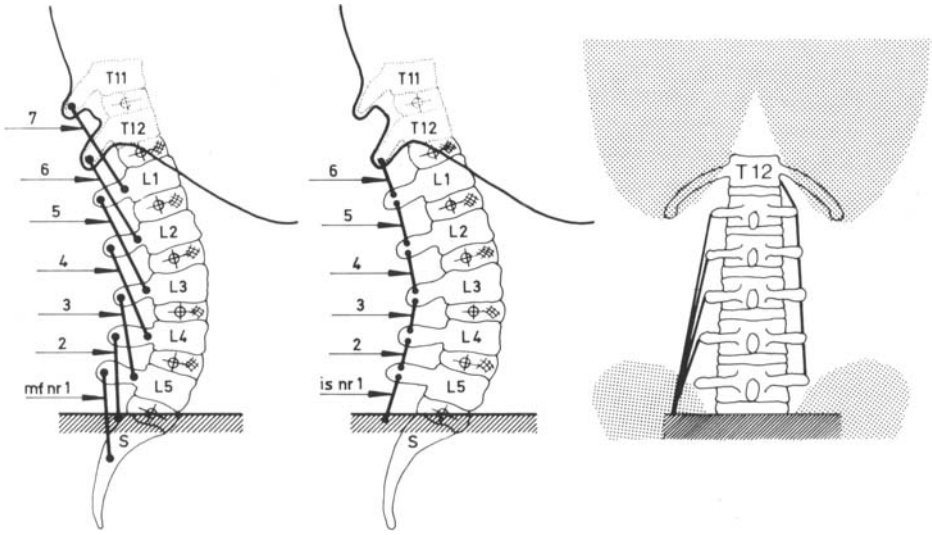

Figure 6-15. The local muscles included in the model.

Left: the multifidi fiber pairs numbered from 1 to 7 starting from the pelvis. Each of the 7 fibers has one left and one right part, originating from the mammilar processes and inserted to the spinous processes of the vertebra two levels above. The first and second multifidi-fibers originate from the sacrum.

Middle: the interspinal muscles.

Right: the left side shows half of the eight quadratus lumborum fibers with origin on the pelvis and insertions on the outermost part of the transverse processes of L1 to L4. The right side shows the five intertransverse fibers connecting the transverse processes of L5 to L1 and L1 to the thoracic cage. The T12-L1 muscle fibers included in the intertransverse group is introduced according to Langenberg (1970). Note that all thoracic vertebrae are included in the thoracic cage, which is considered as a rigid body.

groups are included in the model: the interspinal-, the multifidi-, the intertransverse- and the quadratus lumborum muscles (Figure 6-15).

The global erector spinae muscles are by far the most important back muscles both as regards equilibrium and stability of the spine.

Because of the S-shaped sagittal projection of the spine, local muscles are necessary to maintain sagittal equilibrium of the spinal system. During normal standing the spinal motion segments are supposed to be in — or close to — their neutral positions and the moments carried passively therefore are much smaller than the moments which are carried by the local muscles. Best suited to carry the local moments are the interspinal, the multifidi muscles and the spinalis muscle (in the upper lumbar region) as they have the longest lever arms in the sagittal plane.

Four muscle groups may give lateral support to the spine: the intertransverse muscles, the quadratus lumborum, the transverse abdominal muscles and the local erector spinae muscle fibers. Minor support also may come from the internal oblique muscles via the lateral raphe and the thoracolumbar fascia.

The main local lateral support is assumed to come from the intertransverse, the quadratus lumborum and the local erector spinae muscle fibers. These are modeled as two separate groups: one single-joint group corresponding to the intertransverse muscles and and one multi-joint group corresponding to the quadratus lumborum and the local erector spinae muscle fibers. The single-joint group is referred to as the "intertransverse" muscles and it contains fibers connecting the transverse processes of two adjacent vertebrae. The multi-joint group is referred to as the "equivalent quadratus lumborum" group. The fibers have their origin on the sacrum and their insertions on the outermost tips of the transverse processes of L1 to L4. Note that no fibers connecting the transverse processes of L5 and sacrum are included in the model. In the following, figures are given for activity in the "equivalent quadratus lumborum" which includes action in both or either of the two muscle groups.

Geometrical properties and posture parameters

The exact posture of the lumbar spine and the thoracic cage in the upright position is described by nine geometrical parameters (Figure 6-16).

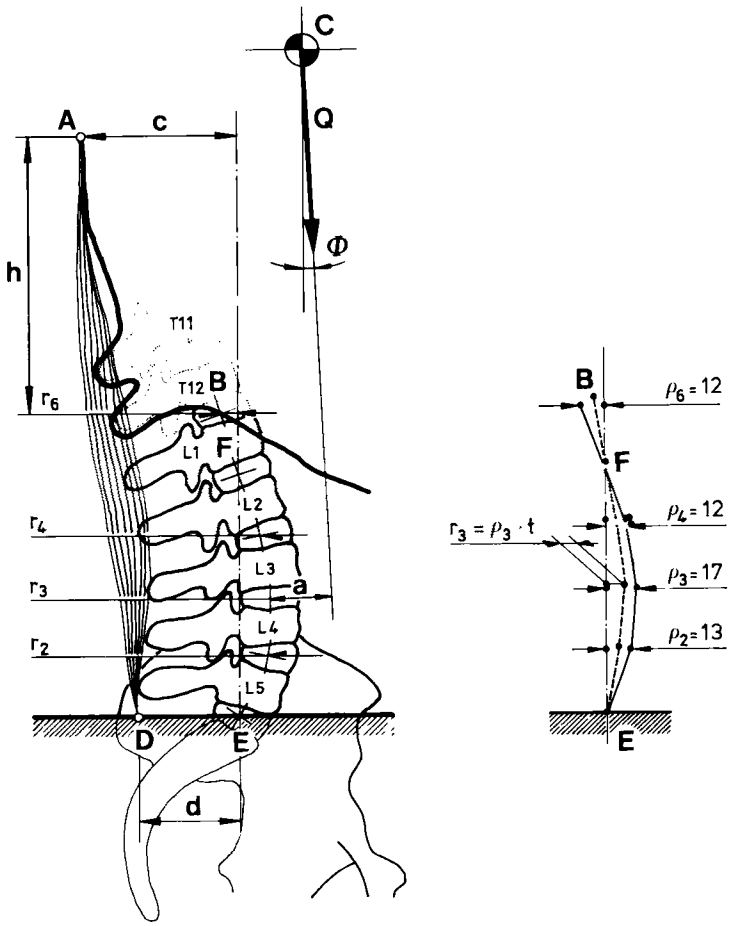

Figure 6-16. The geometrical parameters used to describe posture and position of the gravity line (which is vertical, although it is drawn here at an angle to the sides of the page). A: sagittal projection of the insertion of the global erector spinae muscle, B: T12-L1 disk-midpoint, C: The combined center of gravity of upper-body weight and the weight that constitutes the outer load (Q), D: sagittal projection of the origin of the global muscle, E: L5-S1 disk-midpoint, F: L1-L2 disk-midpoint. The posture of the pelvicspinal-thoracic cage system relative to the EF-line is defined by the parameters r_i, ρ_i and t, the relative lordosis. The distances from the EF-line to the nodes (disk-midpoints) are $r_i = \rho_i \cdot t \cdot \Phi$: inclination of the EF-line relative to the gravity line. a: distance from the most anterior disk-midpoint to the gravity line. The numerical Figures for ρ_i in mm are given to the right. Choice of reference frame is made by putting $\rho_i = \rho_5 = 0$. The coordinates of the global muscle insertions on the thoracic cage (A relative to B) are given by c and h. c = 59 + 21t mm and h = 100 mm. The lateral positions of the insertions are taken as ± 100 mm. The coordinates of the origin D are given by d = 60 mm with the lateral positions ± 70 mm.

The shape of the spine itself is defined by the relative lumbar lordosis, t, and the parameters r_i. For the upright standing posture with no outer load (the system is loaded by the gravity force of the upper body only), the relative lumbar lordosis is specified to t = 1.0. The parameters r_i are measured from an X-ray photo (Schmorl and Junghans 1968) for this position as the distances r_i according to Figure 6-16.

The position of the pelvis, the lumbar spine and the thoracic cage relative to each other is thus uniquely defined by t and r_i. The inclination of this complex with respect to the vertical is given by the angle Φ (Figure 6-16). The position of the gravity line from the combined center of gravity of the upper-body weight and the weight that constitutes the outer load is specified by its distance a from the most anterior disk midpoint.

The distance between the global erector spinae muscle insertion (point A in Figure 6-16) and the upper-body gravity center can be assumed as approximately constant and independent of the shape of the spine (including lumbar and thoracic parts) and consequently also independent of t and Φ. A decreased value of t,

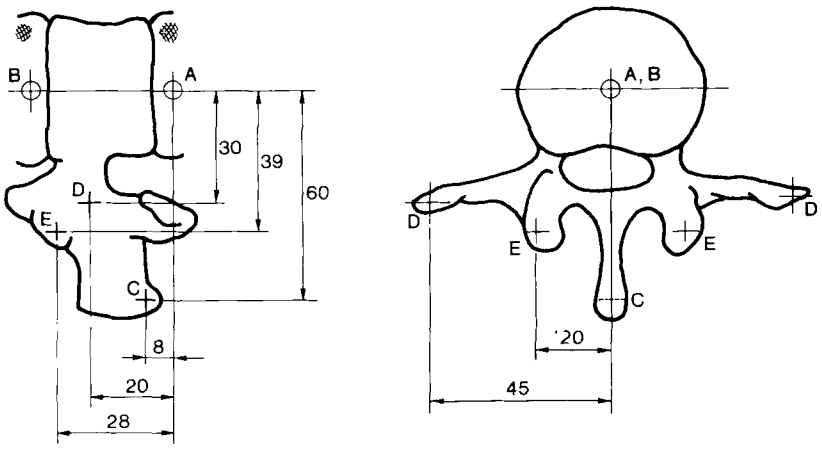

Figure 6-18. Sagittal and horizontal views of the "standard" vertebrae used for modeling of the local muscle attachments. The coordinates are given in mm. A and B: diskmidpoints below and above, C: multifidi muscle insertion to the spinous process, D: quadratus lumborum insertions to the transverse processes, E: multifidi muscle origins on the mammilar processes.

while Φ is kept constant at a sufficient small value, will move the upper-body gravity center in the anterior and the L2-L3, L3-L4 and L4-L5 disk midpoints in the posterior direction with respect to T12-L1, causing an increased value of the distance a. Using the numerical data given in Figure 6-16 the increase Δa can be calculated as a function of t: $\Delta a = (1-t) \cdot 50$ mm.
In the standing posture, a person can increase the distance a in one or more of three ways:

1. moving the outer load forwards (only a is changed),
2. flexing the trunk, (Φ and a are changed) and
3. decreasing the lumbar lordosis (t and a are changed).

All muscle attachment to the elements are modeled as points and are estimations of the center of the real, distributed origins and insertions. The coordinates for origin and insertion of the global erector spinae muscles are given inFigure 6-16. The geometrical properties of the "standard" vertebra used for modeling the local multi-joint muscle attachments are presented in Figure 6-18.

The parameters t and Φ thus uniquely define all multi-joint muscle origins and insertions.

Detailed information of muscle origins and insertions of the single-joint muscles is not necessary. The influence from these muscles (*i. e.* the interspinal-, the intertransverse- and multifidi muscle pairs number 1 and 7) is considered on page 36.

Influence from the thoracolumbar fascia

The tensile force from the thoracic cage to the pelvis possibly carried by the thoracolumbar fascia is neglected. This approximation ought to be reasonable when the standing position with a lumbar lordosis is considered.

The retinaculum formed by the dorsal and middle layers of the thoracolumbar fascia is attached to the transverse processes of the lumbar spine and along the midline at the spinous processes. Obviously it constrains the global erector spinae muscles laterally and sagittally with respect to the lumbar spine. This function is modeled by prescribing the position of each global muscle fiber at certain points. Thus at each of 5 disk-midpoint levels (horizontal planes through the disk-midpoints L4-L5 to T12-L1), the global muscle fibers are assumed to pass through a point which is rigidly connected to the vertebra below. In this way the global muscle fibers follow curved paths. The points can be considered as symmetrically placed rings through which the muscle fibers pass. The geometrical properties of the curved path prescribed are given in Figure 6-19.

In order to examine the role of the thoracolumbar fascia, calculations are made with as well as without considering its constraining action. Thus both a "curved path model" and a "straight path model" is studied.

The curved path is specified for the global erector spinae muscles, only. All other muscles are modeled as straight path muscles.

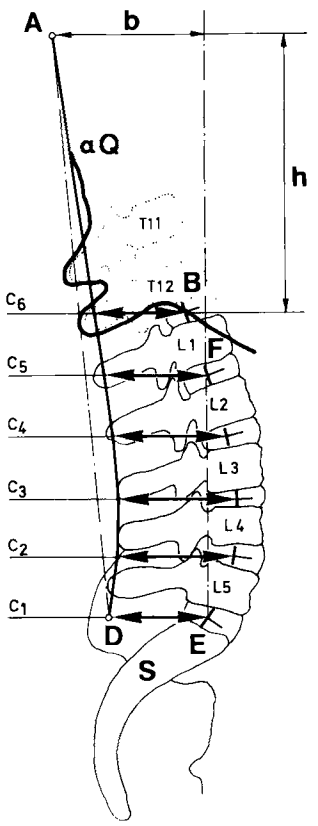

Figure 6-19. Sagittal view of the two different ways of modelling the global erector spinae muscles. A: muscle insertion, B: T12-L1 disk midpoint, D: muscle origin, E: L5-S1 disk-midpoint, F: L1-L2 d:o. The straight point line AD shows the "straight path model" and the full drawn AD line defined by the breakpoints at the distances c_1 to c_6 from the disk-midpoints shows the "curved path model". $c_1 = 60$ mm, $c_2 = 58 + 7.7t$, $c_3 = 56 + 10.9t$, $c_4 = 54 + 14.4t$, $c_5 = 52 + 4.8t$ and $c_6 = 50$ mm. The frontal projections of the two models are the same, *i.e.* they show straight lines from the muscle origins at ±70 mm on the pelvis to the insertions at ±100 mm on the thoracic cage.

Motion segment torque stifnesses

The great differences of the motion segment torque stiffnesses reported in the literature (Markolf 1972), see further the discussion in Chapter 4, are taken into consideration by using figures for the torque stiffnesses in the range found.

In all deformation modes, the stiffnesses are nonlinear — increased rotation gives increased stiffness. For lateral bending and axial rotation, the nonlinear behavior need not to be considered here as the initial posture always corresponds to zero rotation for the motion segment. In flexion-extension, however, this simple approach is not possible. Due to the nonlinear characteristic, the value of the relative lordosis t will influence the flexion torque stiffness. A decreased relative lumbar lordosis corresponds to an increased flexion angle of the motion segments. The mean value for the flexion stiffness found by Markolf was $\lambda_{so} = 1.8$ Nm/degree. This figure is taken as the 'normal' stiffness for t = 1.0. For t = 0.5, the normal stiffness is taken as 3.6 Nm/degree and for t = 0.3 as 4.5 Nm/degree. These latter two stiffnesses are very rough estimations. As will be shown later in the result sections, however, the importance of the magnitude of the passive flexion-extension stiffness decreases for increased vertical loading. The combination of high vertical loading and a flat back (low t-value) is therefore well described by the model.

The flexion-extension stiffness used for different t-values are (with "normal" values cursive):

t = 1.0 : λ_{so} = 0.9, *1.8* and 3.6 Nm/degree,
t = 0.5 : λ_{so} = 1.8 and *3.6* Nm/degree,
t = 0.3 : λ_{so} = 3.6 and *4.5* Nm/degree.

For t = 1.0 thus a soft and a stiff back is modeled. For t = 0.5 and t = 0.3, a normal and a soft back is modeled.

The axial rotation torque stiffness is set at 13 Nm/degree corresponding to the mean value found by Schultz et al. (1970). To investigate the influence of λ_{ro}, runs were made for λ_{ro} in the range 1.25 to 30 Nm/degree for one loadcase.

In lateral bending, the mean torque stiffness found by Markolf was 1.3 Nm/degree with variations from 0.5 to 3 Nm/degree for L1-L2 to L5-S motion segments and from 1.5 to 4.5 Nm/degree for T12-L1 motion segments. In the model, the lateral torque stiffness is set equal for all levels. The underestimation of the stiffness of the T12-L1 motion segment shall be seen as a compensation for the overestimation of the stiffness above when the thoracic cage is modeled as a rigid body.

The lateral bending stiffness of the local system is found to be crucial. The results indicate that local lateral support is always necessary. The calculations are made for $\lambda_{lo} = 1.3$ Nm/degree which is the mean value found by Markolf. Larger lateral bending stiffnesses can be treated by using the equivalence between bending stiffness and a certain contribution from the activity in the intertransverse muscles. See further page 36.

Muscle stiffnesses

Each muscle fiber included is modeled as a linear spring with the stiffness proportional to the muscle force divided by the muscle length according to eqn. 6.2. The muscle forces are either given fixed values (parameters) or they are calculated to fulfill to conditions for equilibrium. The muscles lengths are taken as the lengths between origins and insertions of the muscles with a few exceptions. The length of the global erector spinae muscle is taken as 300 mm, which is shorter than the distance from origin to insertion in the model. The origin of this muscle is on the erector spinae aponeurosis and the length used is an estimation of the real muscle fiber length.

In the model only short (two segment) multifidi muscles are included. In reality the load probably is shared between short and long multifidi muscle fibers. The modeling of the multifidi muscle fibers therefore leads to an overestimation of the stiffness contribution from these muscles. Therefore the stiffness of the multifidi muscles is reduced by 50% for most of the calculations. A few runs are made without reduction in order to investigate the influence of the multifidi muscle stiffness.

Reduction of the system to static determinateness

First of all it must be stated that the model created is highly statically indeterminate. In spite of the fact that the system contains far from all muscles in a real spinal system, there are in total 40 individual muscle fibers included (17 pairs and 6 mid-sagittal interspinal fibers) and thus also 40 unknown muscle fiber forces. Considering the fact that only symmetric loading is regarded implies that the forces in each pair are equal and thus the number of unknown forces is reduced to 23. In each of the six intervertebral disks included, two forces, the compression and the shear force, as well as the bending moment passively carried by the motion segment, are unknown. The total number of unknown quantities thus amounts to 41.

At each of the six lumbar levels three equations of equilibrium are available, thus in total 18 equations. This means that the number of unknown quantities far exceeds the number of equations. To be able to treat this indeterminate system, several assumptions are made. In addition to the outer load (Q), the forces in three muscle groups, the global erector spinae (Fg), the quadratus lumborum and the intertransverse muscles, are treated as independent variables *i. e.*they are given fixed values for each run. Each of the eight fiber forces in the quadratus lumborum group is given the same, specified, value called "Fql, etc", and each of the ten fiber forces within the intertransverse muscle group is given the same, specified, value called "Fit". The choice of Fit is related to an assumption of maximum possible intertransverse muscle force and it is made as described below. The choice of Fql, etc is rather arbitrary and different sets of reasonable values are chosen.

It is assumed that the moments carried passively by the six motion segments are small compared to the moments carried by the muscles and they are therefore neglected.

There now remains 13 unknown muscle fiber forces (7 multifidipairs and 6 interspinal) and 12 unknown forces on the disks (the compressive and the shear force at each of the six levels), *i. e.* in all 25 unknown forces and as only 18 equations of equilibrium are available, the system is still statically indeterminate.

Two more assumptions are therefore made to make it possible to solve the problem:

First an assumption on the force distribution between the interspinal and the multifidi muscles based on their relative transverse muscle areas. Secondly an assumption on the force distribution within the multifidi fibers (Bergmark 1987, page 73).

In this way, seven more equations are available and the system is now uniquely solvable.

Table 2. Musclefiber length and lever arms (mm) used to calculate the joint stiffness contribution

Muscle	Action	Length	Lever arm
Interspinal	sagittal	25	50
Intertransverse	lateral	25	40
	sagittal	30	
Multifidi No 1	sagittal	70	60
Multifidi No 7	sagittal	160	35

Influence from the single joint muscles

The single-joint muscles included in the model are: the interspinal- and the intertransverse muscles and multifidi muscle pairs number 1 and 7 (Figure 6-15). The stiffness contribution from a single-joint muscle is calculated according to eqn. 6.5. First the individual muscle forces are calculated according to the previous section. The data from Table 2 for the musclefiber length and the lever arms are used to calculate the joint stiffness contribution.

Maximum value of the intertransverse muscle force, Fit_{max}, is estimated by assuming a transverse muscle area of $A = 2*0.5\,cm^2$ (I have not found any data in the literature). The physiological limit for the muscle stress, σ, (force per unit muscle area) is ranging from σ = 0.4 to 0.8 MPa (Ikai et al. 1968). One obtains $Fit_{max} = A \cdot \sigma = 2*20$ to $2*40$ N acting over each disk-midpoint level. In this investigation, lateral stability is evaluated for Fit = 0, 5.6, 11.2 and 22.4 N in each of the 10 intertransverse muscle fibers. The Fit-values are chosen in order to give the lateral stiffnesses $\lambda_1 = 0, 0.5$, 1.0 and 2.0 Nm/degree for q = 40 according to eqn. 6.5.

Critical global erector spinae muscle activity a_c

The condition for equilibrium implies that the resulting moment from the outer load (Q) at each intervertebral disk level is counteracted by muscle activity in the back muscles.

All back muscles act posteriorly to the intervertebral disk-midpoints which in turn implies that the gravity line for Q must always pass anteriorly to the disk midpoints.

For each (given) set of the intertransverse (Fit) and equivalent quadratus lumborum (Fql, etc) muscle forces, equilibrium can be maintained for fixed combinations of muscle forces in the local sagittal (interspinal and multifidi) system and the global (erector spinae) system. The force distribution between these two systems are given by the parameter α. For $\alpha = 0$, equilibrium is maintained by muscle forces in the local system only. For increased α, the muscle forces are moved from the local sagittal to the global system.

There is, however, an upper limit for α, here called α_c, when one or more of the muscle forces in the local sagittal system are zero. A further increased α would imply negative (compressive) muscle forces in the local system to maintain equilibrium at the given posture. For $\alpha > \alpha_c$ extension of the spine occurs.

It is here assumed that the passive moment carried by the motion segment is zero. This is strictly true for one specific value of the relative lumbar lordosis t. However, for other values of t, this passive moment is certainly very small compared to moments from individual muscles and it can safely be neglected (as also mentioned on page 36), even though its relative influence can be tangible at very low outer loads.

Muscle stress (force per unit area) in the local and global systems

The solutions obtained from the stability analysis will show the region in which mechanical stability prevails. However, this is not the only criterion for physiologically possible solutions. Therefore also the muscle stress (force per unit area) in the global and the local systems are calculated.

The stress in the global erector spinae muscle is:

$$\sigma_g = \alpha Q / A_g \qquad (6.11)$$

where αQ is the muscle force and A_g is the transverse area of the active part of the muscle. The total transverse area of the erector spinae muscle is about 36 cm^2. This figure is obtained from measurements on the original photographs from the investigation by Jonsson (1970). According to Bogduk and MacIntosch (1984), two thirds of the erector spinae area belongs to the global fibers and A_g is therefore taken as 24 cm^2.

The moment carried by the local sagittal system (the multifidi, the interspinal and in the upper lumbar region also the spinalis muscles) is for $\Phi = 0$ maximum at the T12-L1 level. For levels below, the moment reaches a minimum at the L3-L4 level and then increases again to another extreme value at the L5-S1 level. For increasing values of Φ, the moment carried at the T12-L1 level decreases and the moment carried at the L5-S1 level increases. Use of a rough estimation of the transverse areas of the local sagittal muscles at the two levels indicates that the corresponding muscle tensions are equal at $\Phi \approx 2.5$ degrees. The local sagittal muscle tension will therefore be calculated for this Φ-value at the L5-S1 level (level 1) for the two heavy loadcases. For normal standing with no outer loads, $\Phi = 0$ will be used.

For $\alpha = \alpha_c$, the moment carried at the L3–L4 level is zero. No local multifidi muscle fiber passing this level is activated in this case and consequently the moment at the L5-S1 level must be carried by multifidi fibers inserted to the spinous processes of the L4 or the L5 vertebrae. This is in accordance with the assumptions already made for force distribution in the local sagittal system as only two-segment multifidi muscle fibers are included. For $\alpha < \alpha_c$, the moment carried at the L3-L4 level increases and therefore multifidi fibers passing this level with origin on the pelvis may be activated. This means that the "activated"part of the local sagittal system at the L5-S1 level may increase. Here, however, the muscle tension at level 1 is calculated for the same force distribution as is used for the stability analysis which implies that the moment M_1 is carried

by the same muscle fibers independent of α. This leads to somewhat overexaggerated local sagittal muscle tensions for $\alpha < \alpha_c$.

The numerical figures used for the tension calculations in the local sagittal system are: $d_1 = 5{,}5$ cm and $A_1 = 6\ cm^2 A_1$ is taken as about half the area occupied by interspinal and multifidi muscle fibers at the L5-S1 level from the investigation by Langenberg (1970).

The muscle tensions obtained shall be compared to the physiological limit. In an investigation by Ikai and Fukunaga (1970) figures in the range 0.4 to 0.8 MPa with mean value of 0.63 MPa were obtained as maximum strength of biceps brachii. In lack of muscle tension limit for the back muscles, the results will be compared to this figure. In order not only not to exceed the muscle capacity but also to avoid muscle fatigue, the allowed muscle tension must be even less. According to recent investigation by Parnianpour et al. (1987) a back muscle force of 80 % of the voluntary maximum value can be maintained for about 1 minute and 60 % of the maximum force for about 2 minutes.

Loadcases considered

The critical situation as regards the mechanical stability of the spinal system is vertical loading on the thoracic cage in the standing posture.

The exact posture depends on the lordosis (which turns out to be dependent on the load magnitude) and on the inclination of the upper body as a whole. The numerical description of the posture is made by means of seven parameters, ρ_2, ρ_3, ρ_4, ρ_6, t, a and Φ (Figure 6-16). For each individual ρ_i are fixed lengths, whereas t, a and Φ vary with changes of the posture. A male person with a length of 178 cm and a weight of 75 kg is considered. The upper-body weight carried by the spinal system is taken as half the total body weight. The center point of gravity of the weight is assumed to act at a height of 175 mm above the T12-L1 level.

Three loadcases are considered:

1. Upper-body weight of 370 N only,
2. upper-body weight plus 400 N extra outer load, and
3. upper-body weight plus 1000 N extra outer load.

The two first loadcases are chosen in order to enable direct comparison with experimental data presented in the literature. The third case corresponds to a very heavy loadcase near maximum capacity.

In loadcase number one (normal standing with no loads) the muscle forces and muscle tensions in the global and local systems are small and will not cause any severe restrictions on the possible configurations of the "standing posture". Thus variations of the lordosis within wide limits do not lead to overstraining of muscle fibers.

In the second and third loadcases, however, depending on the lumbar lordosis, the muscle tensions in individual muscle fibers of the local system may be very large. In these cases the possible variations of the posture are small, since only postures leading to muscle activity patterns with reasonably low muscle tension levels can be accepted.

Method used to solve the problem

The problem to be solved is to find the condition on the muscle stiffness coefficient q, which gives a *stable* equilibrium at a specific posture, *i.e.* the potential energy of the system shall have a minimum. The method used to solve the problem is thoroughly described in Bergmark (1987).

7. Results

The results will be presented in two ways: "complete stability" diagrams and "posture-activity" diagrams.

The concept of the complete stability diagram has been shown earlier in Figure 6-13. For a given posture (t, Φ and a; Figure 6-16), loading (Q) and force in the laterally stabilizing local muscles (Fit and Fql, etc.), the diagram shows the necessary conditions to maintain mechanical stability of the spinal system. A typical result is presented in Figure 7-1. Mechanical stability can be maintained if the muscle stiffness coefficient q is larger than than the critical value q_{crit}. The degree to which the global system is activated, is represented by the dimensionless quantity α which is the global muscle force divided by the outer load (see page 30). The diagram shows influence from two deformation modes: one characterized by coupled lateral bending–axial rotation and the other by flexion–extension. If instability occurs under the coupled lateral bending–axial rotation mode, then, as an inspection of the eigenvectors shows, the instability deformation will be dominated by lateral bending. The coupled lateral bending–axial rotation will therefore in the following be referred to as "lateral bending" mode only. The flexion–extension mode will be referred to as the "sagittal" mode.

From the stability diagram the following conclusions can be drawn:

Equilibrium is maintained for all $\alpha < \alpha_c$ by appropriate action of the local system.

Loss of sagittal stability sets the lower limit for q.

For a fixed value of q, above the lower limit, there exists a lower and an upper bound for α to maintain mechanical stability of the system.

The lower bound for α is based on the demand for lateral stiffness.

In the example shown (Figure 7-1), for q = 40, the lower bound for α is $\alpha_1 \approx 0.17$. The upper bound for α is $\alpha_c \approx 0.24$. One observes that for q less than about 37, stability at the given posture is not possible at all.

The value of the muscle stiffness coefficient q is not accurately known. From experimental data presented in the literature, q is estimated at about 40 (Bergmark 1987, Appendix 2). The qualitative behavior of the model is however not critically dependent on the exact value of q.

The second type of diagram used to present the results is the "posture-activity" diagram. This diagram is obtained by combining several complete stability diagrams for different a-values and assuming that a fixed value of q exists. The diagram gives a description of the situation in which a *posture control* system may work. It shows, for fixed values of q, Q, Fql, etc. and Fit, the values of α for which mechanical stability can be obtained as a function of the position of the gravity line, a, and the relative lordosis t. The posture-activity diagram for loadcase 1 with Fql, etc. = 8*5 N and Fit = 10*5.6 N (corresponding to a lateral stiffness of λ = 0.5 Nm/degree according to eqn. 6.5) is shown in Figure 7-2 for q = 40. The diagram is valid for Φ (inclination of the trunk) equal to zero. It will, however, later be shown that the influence of a variation of Φ within ± 5 degrees on the stability is small and consequently the posture-activity diagram in Figure 7-2 is influenced by changes of Φ to a minor degree only. As is discussed in chapter 6 (page 32), the distance a may be increased in either of three ways: by leaning a little forward, by

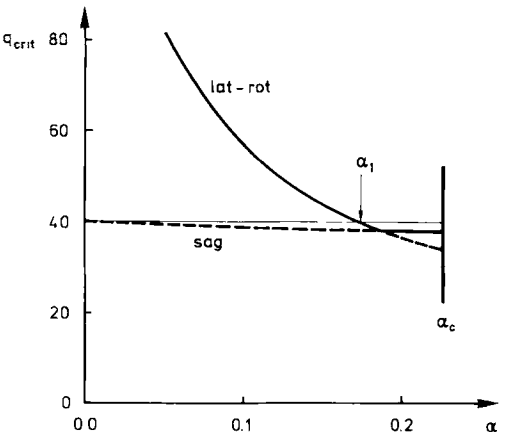

Figure 7-1. The complete stability diagram for loadcase 1, *i.e.* normal standing posture with no outer load, a = 22.5 mm, t = 1.0, F = 0 and cmf = 0.5. q_{crit} is given for $\lambda_{lo} = 1.3$, $\lambda_{so} = 1.8$, $\lambda_{ro} = 13.0$, Fit = 10*5.6 N (corresponding to λ = 0.5 Nm/degree) and Fql, etc. = 8*5 N. In the diagram, the condition for lateral–rotational and sagittal stability are shown. Stability prevails if the muscle stiffness coefficient $q > q_{crit}$ according to the full drawn line. Regardless of q, equilibrium cannot be satisfied if $\alpha > \alpha_c$. If, for example, q = 40, the stability can be maintained for $\alpha_1 < \alpha < \alpha_c$. One also observes that stability at the given posture and values of Fit and Fql, etc. cannot be maintained if q is less than about 37.

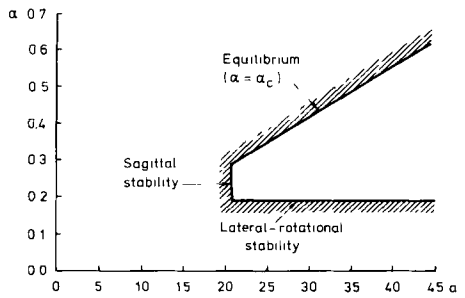

Figure 7-2. Posture-activity diagram for loadcase 1, q = 40. The diagram shows the three limits for allowed combinations of the global muscle activity α and the posture parameter a: the lateral–rotational and sagittal stability limits and the equilibrium limit. λ_{lo} = 1.3, λ_{so} = 1.8 and λ_{ro} = 13.0, Fit = 10*5.6 N (corresponding to λ = 0.5 Nm/degree) and Fql, etc. = 8*5 N.

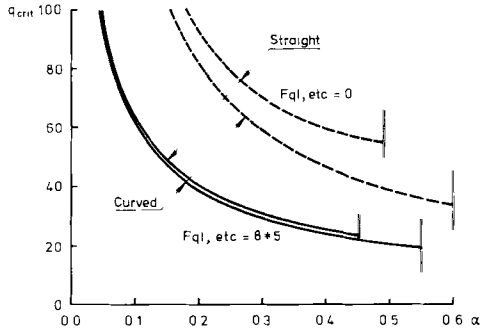

Figure 7-3. Lateral stability diagrams for loadcase 1, a = 40 mm. Straight path (dashed lines) and curved path stabilization (full drawn lines). cmf = 0.5, λ_{lo} = 1.3, λ_{so} = 1.8 and λ_{ro} = 13 Nm/degree. Fit = 0 and Fql, etc. = 0 and 8*5 N. The vertical lines indicate α_c. Each line terminates at $\alpha = \alpha_c$.

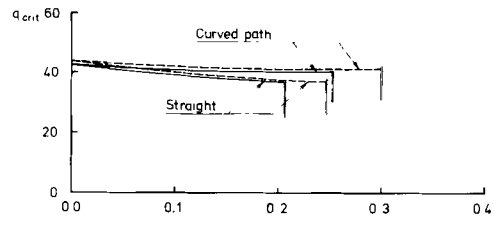

Figure 7-4. Sagittal stability diagrams for loadcase 1, straight and curved path stabilization. a = 20 mm. Notations and remaining parameter values: see Figure 7-3.

moving the load forwards or by decreasing the lumbar lordosis. The diagram in Figure 7-2 is valid for upper body weight only at a fixed t-value. In this case the value of a is changed by Φ only.

Loadcase 1. Upper-body weight only

The two diagrams already shown are valid for loadcase 1.

The influence of the two different ways to model the global erector spinae muscles, "straight path" and "curved path" models as described on page 34, are shown in Figure 7-3 (lateral stability) and 7-4 (sagittal stability).

From diagram 7-3, it is seen that straight path stabilization is less efficient than curved path stabilization in the lateral direction. One also observes that α_c is lower for straight path stabilization which is a consequence of the difference in lever arms for the global erector spinae muscle for the two stabilization models (see also Figure 6-18). The influence from Fql, etc. on the lateral stability is notable. From the figure it is also seen that the difference in lateral stability between the straight path and curved path models is more pronounced when no additional stabilization influence from the local system is present. For Fql, etc. = 8*5 N, the difference between the two models mainly concerns the magnitude of α_c.

Sagittal stability (Figure 7-4) is slightly more easily obtained for the straight path model. However the differences are small. The influence from Fql, etc. on the sagittal stability is small. (Note that Figure 7-3 is valid for a = 40 mm and Figure 7-4 for a = 20 mm.)

With a q-value of about 40, it is obvious that stability during normal standing without recruiting lateral stabilizing muscles is not possible for the straight path model at a = 40 mm or less. For the curved path model, lateral stability is obtained for α greater than about 0.5 (which, as is seen from Figure 7-9, demands a minimum a-value of about 32 mm).

From the diagrams, two conclusions concerning the influence of the thoracolumbar fascia can be made:

1. The fascia gives the spine lateral support. The importance of this is small when also direct local lateral support is present.

2. For a given value of the distance a, a higher global erector spinae activity α_c is allowed.

It is judged that the curved path model gives results closer to the real behavior of the spinal system and in the rest of this investigation only this model will be considered.

For each loadcase, there are six variables involved in the system, a, Φ, t, α, Fit and Fql, etc.. In addition, since the values of the five parameters q, cmf, λ_{lo}, λ_{so} and λ_{ro} are rather uncertain, the analysis has been performed with different choices of the values of the parameters. In the complete stability diagrams, α is the independent and q the dependent variable. In the posture

–activity diagrams, a is the independent and α the dependent variable. q is specified to 40 for these diagrams.

Both types of diagrams may, quite naturally, in some cases look rather confusing due to the many parallel choices of some of the parameters. However for the qualitative understanding of the system detailed information of the relative influence of different parameters may not be necessary. Therefore diagrams will also be presented for one specific "best choice" set of the parameters. For loadcase 1, this is already made in Figure 7-1 and 7-2. The "best choice" parameter set for loadcase 1 and t = 1.0 is chosen as q = 40, cmf = 0.5, λ_{lo} = 1.3, λ_{so} = 1.8 and λ_{ro} = 13 Nm/degree.

The influence of Φ, *i.e.* the inclination of the spinal system relative to the gravity line, is shown in Figure 7-5 for $\Phi = \pm 5$ degrees. The influence on the lateral and the sagittal stability is small and for the rest of the investigation, $\Phi = 0$ will be used only.

The influence of Fit and Fql, etc. on the sagittal stability is shown in Figure 7-6. From the diagram it is seen that the influence on q_{crit} is small. Because of the sagittal moment induced by the interspinal and the quadratus lumborum muscle fibers, increased activity in these two muscle groups gives a lower α_c. For the examples shown, $\alpha_c \approx 0.3$ when no activity in the interspinal and the quadratus lumborum muscles is present and $\alpha_c \approx 0.23$ for Fit = 10*5.6 N (corresponding to lateral stiffness of λ = 0.5 Nm/degree for q = 40) and Fql, etc. = 8*5 N.

The influence of the multifidi coefficient cmf is presented in Figure 7-7. The diagram shows the sagittal stability curves for cmf = 0.5 and 1.0. For $\alpha = 0$, the sagittal stability is entirely maintained by the local system. For increasing α, the local muscle forces and thus also the local stiffnesses, decrease. From the diagrams one observes that q_{crit} is approximately constant and independent of α which indicates that the decreased local stability is almost compensated by the increased sagittal stiffening influence from the global erector spinae muscles. The sagittal stability is, of course, more easily obtained for cmf = 1.0 than for cmf = 0.5, as cmf simply is a measure of how much of multifidi muscle stiffness that is taken into consideration in the calculations. For α close to α_c, the difference is, however, small. The condition for lateral stability actually demands α-values close to the upper limit, and therefore the actual value of cmf is not critically important for the qualitative behavior of the system. For most of the remaining diagrams, cmf = 0.5 will be used.

The influence on the lateral stability from the parameter cmf is very small. No diagram is shown as the difference would not be visible on the scale to which they are drawn.

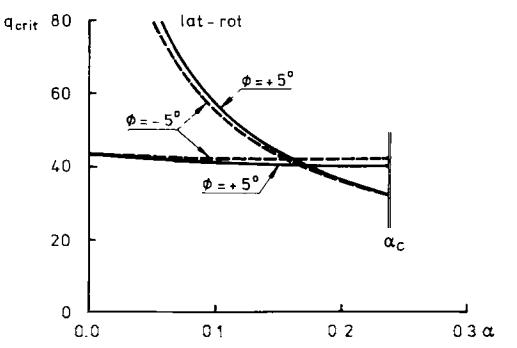

Figure 7-5. Complete stability diagrams for loadcase 1, *i.e.* normal standing with no outer load. Influence of the inclination Φ. Lateral and sagittal stability, a = 20 mm, Fit = 10*5.6 N (corresponding to λ = 0.5 Nm/degree for q = 40) and Fql, etc. = 8*5 N. Full drawn lines: λ = +5 degrees, dashed lines: λ = -5 degrees.

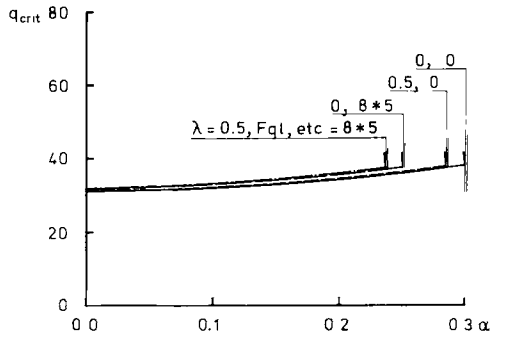

Figure 7-6. Sagittal stability for loadcase 1, a = 20 mm. Influence of the interspinal- (Fit) and the quadratus lumborum muscles (Fql, etc.). Full drawn lines: Fit = 10*5.6 N (corresponding to λ = 0.5 Nm/degree for q = 40) and Fql,etc. = 8*5N. Short dashed lines: Fit = 0, Fql,etc. = 8*5. Long dashed lines: Fit = 10*5.6 N, Fql, etc. = 0. dashed-dotted lines: Fit = 0 and Fql, etc. = 0. Each line terminates at $\alpha = \alpha_c$.

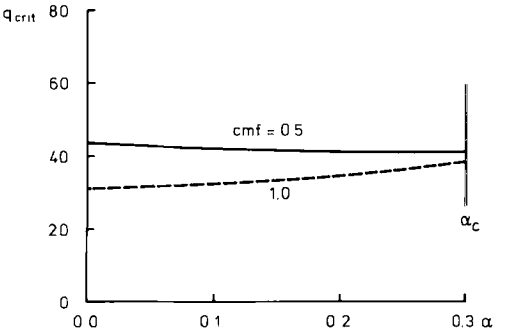

Figure 7-7. Sagittal stability diagram for loadcase 1, a = 20 mm. Influence of the multifidi coefficient cmf. Lateral and sagittal stability curves are shown for cmf = 0.5 and 1.0. λ_{lo} = 1.3, λ_{so} = 1.8 and λ_{ro} = 13 Nm/degree.

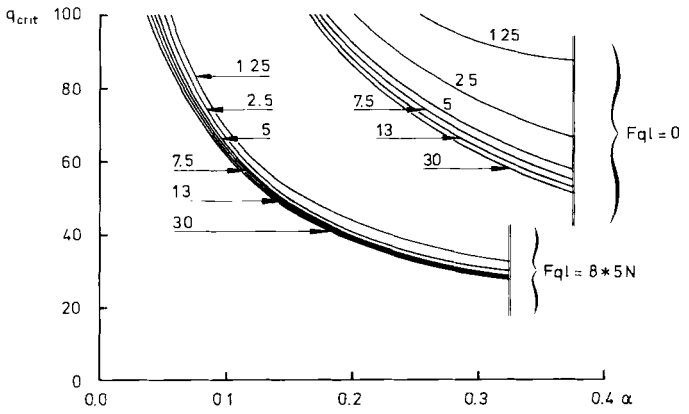

Figure 7-8. Lateral stability diagram for loadcase 1, a = 25 mm. λ_{ro} = 1.25, 2.5, 5, 7.5, 13 and 30 Nm/degree. Fit = 0. Upper curves: Fql, etc. = 0. Lower curves: Fql, etc. = 8*5 N.

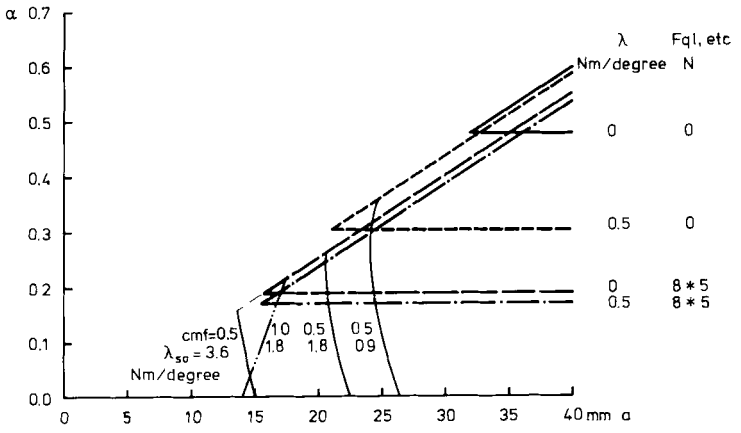

Figure 7-9. Loadcase 1. Posture-activity diagram for q = 40. Influence of the sagittal and lateral passive motion segment torque stiffnesses. λ_{so} = 0.9, 1.8 and 3.6 Nm/degree. The sagittal stability are given for cmf = 0.5 (λ_{so} = 0.9, 1.8 and 3.6 Nm/degree) and for cmf = 1.0 (λ_{so} = 1.8 Nm/degree only). λ_{ro} = 13 Nm/degree. The Fit - Fql, etc. combinations used are: 0 - 0, 10*5.6 - 0, 0 - 8*5 and 10*5.6 N - 8*5 N.

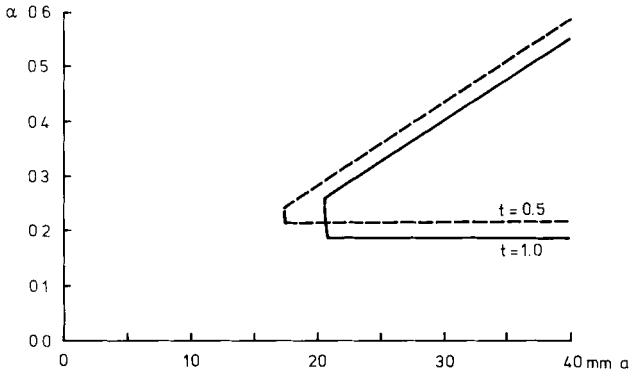

Figure 7-10. Loadcase 1, posture-activity diagrams for t = 1.0 and t = 0.5. The diagrams are valid for the "best choice" parameter set, i.e. λ_{lo} = 1.3, λ_{ro} = 13, for t = 1.0, λ_{so} = 1.8 and for t = 0.5, λ_{so} = 3.6 Nm/degree. Fit = 0 and Fql,etc. = 8*5 N.

The influence of the passive axial rotation motion segment stiffness, λ_{ro} is presented in diagram 7-8. This parameter influences the lateral-rotational stability only. Remember that the deformation mode at "lateral instability" in the calculations show a combination of lateral bending and axial rotation. For λ_{ro} of the order 5 to 30, the lateral bending of the motions segments dominate. For lower λ_{ro} values, there is also a pronounced axial rotation at the instability mode. The stability curves for λ_{ro} = 1.25, 2.5, 5, 7.5, 13 and 30 Nm/degree are shown for Fit = 0, Fql, etc. = 0 and 8*5 N. As in the case shown in Figure 7-3 one observes the remarkable influence of Fql, etc. on lateral stabilization. The influence on the lateral stability from changes in λ_{ro} is greater when no lateral stabilization from the local system is present. To maintain lateral stability for q = 40 at a = 25 mm, the laterally stabilizing local system must be activated and in this case the influence from changes in λ_{ro} of the order from 5 to 30 Nm/degree is small.

In Figure 7-9, the posture-activity diagram for loadcase 1 is shown. From the diagram it is seen that the minimum value of the distance a for which stability is possible is primarily dependent on Fit and Fql, etc.. Provided the local lateral support is high enough, the minimum value of a for which stability is possible is set by λ_{so}. For λ_{so} = 1.8 Nm/degree (which equals the mean value found by Markolf 1972), the minimum a-value is about 21 mm. For λ_{so} = 3.6 Nm/degree the minimum a-value is about 14 mm (which demands a higher local lateral support than is shown in the Figure) and for λ_{so} = 0.9 Nm/degree, the minimum a-value is about 25 mm. All α_c-lines are parallel. The different α_c for a given a-value are caused by the influence on the sagittal equilibrium from the intertransverse and quadratus lumborum muscles.

From the diagram in Figure 7-9, one also observes that the condition for lateral stability is independent of the distance a and depending on the global activity α and the local lateral support only. When a is changed for given values of α, Fql, etc. and Fit, the forces in the multifidi muscles and the interspinal muscles will change. Obviously these two latter muscles have no influence on the lateral stability of the system. The multifidi and interspinal muscles have a sagittal action only and it is therefore adequate to introduce the term "local sagittal system" for these muscles. Returning to Figure 7-6, it is seen that the influence on the sagittal stability from the intertransverse and the equivalent quadratus lumborum muscles is small. These muscles have a mainly lateral action and consequently they may be called the "local lateral system".

The influence from the relative lordosis t on the stability is shown in Figure 7-10. The Figure shows the posture-activity diagrams for t = 1.0 and t = 0.5. The figure is valid for the "best choice" set of parameters, Fit = 0 and Fql, etc. = 8*5 N. From the figure it is seen that the influence from t is small. The increased flexion stiffness of the motion segments gives the spinal system an increased sagittal stiffness which allows a minimum a-value of about 17.5 mm for t = 0.5 compared to a minimum a-value of about 21 mm for t = 1.0. A slight increase in α_c is obtained for t = 0.5 due to the shorter lever arms for the global erector spinae muscle, see Figure 6-18. The same local lateral support is assumed for both t-values and from the figure it is seen that lateral stability is more easily obtained for t = 1.0 than for t = 0.5.

Loadcase 2. Upper-body weight plus 400 N carried on the shoulders

In this case, the vertical load acting on the thoracic cage will be the combination of gravity forces (370 N) acting at the center of gravity of the upper body (assumed to be placed 175 mm above the T12-L1 disk-midpoint) and the force 400 N from a weight attached at the shoulder level (assumed to be 290 mm above the T12-L1 joint). The combined load is 770 N acting at a vertical height of 235 mm.

Due to the increased flexion-extension torque stiffness when the lumbar lordosis decreases, i.e. for a flatter back, the best choice values are chosen as λ_{so} = 1.8 Nm/degree for t = 1.0 and λ_{so} = 3.6 Nm/degree for t = 0.5.

The complete stability diagram for a = 35 mm and relative lordosis t = 0.5 is presented in Figure 7-11. The

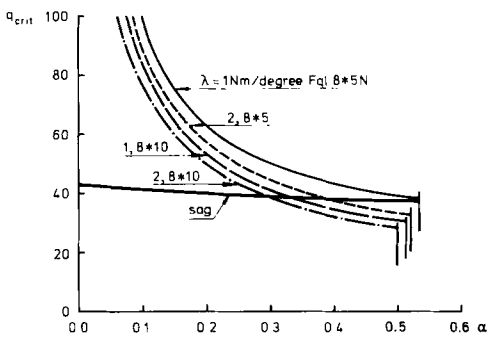

Figure 7-11. Complete stability diagram for loadcase 2, 400 N carried on the shoulders, relative lordosis t = 0.5 and a = 35 mm. λ_{lo} = 1.3 and λ_{ro} = 13 Nm/degree. $\Delta\lambda$ = 1 and 2 Nm/degree (corresponding to Fit = 10*11.2 N and 10*22.4 N), Fql, etc. = 8*5 and 8*10 N. The influence from Fit and Fql, etc. on the sagittal stability is small and is not seen in the diagrams at the scale in which they are drawn.

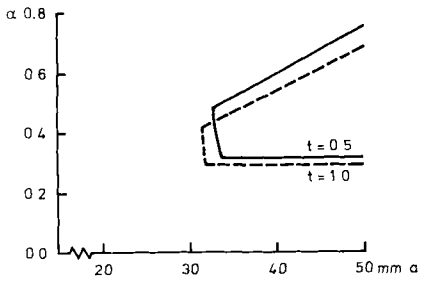

Figure 7-12. Loadcase 2, posture-activity diagram for q = 40, t = 0.5, Fit= 10*11.2 and 10*22.4 N (corresponding to λ = 1.0 and 2.0 Nm/degree), Fql, etc. = 8*5 and 8*10 N. λ_{so} = 1.8 and 3.6 (best choice) Nm/degree. cmf = 0.5, λ_{lo} = 1.3 and λ_{ro} = 13 Nm/degree.

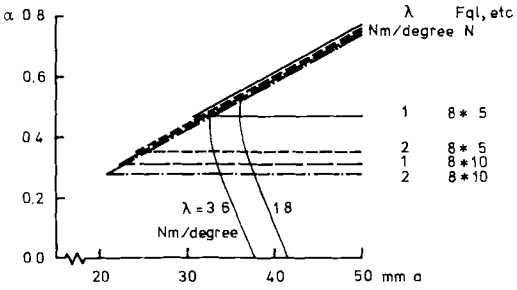

Figure 7-13. Loadcase 2, posture-activity diagram for q = 40. Comparison of conditions for relative lordosis t = 0.5 and t = 1.0. Full drawn lines: t = 0.5, λ_{so} = 3.6 Nm/degree, dashed lines: t = 1.0, λ_{so} = 1.8 Nm/degree. Fit = 10*11.2 N (λ = 1.0 Nm/degree) and Fql, etc. = 8*10 N.

mechanical behavior of the system is essentially the same as in loadcase 1. Limitations of lateral stability, sagittal stability and equilibrium are represented by curves with the same principal character. From the diagram it is seen that for this posture and q = 40, a minimum activity in the local lateral stabilization system corresponding to Fit = 10*11.2 N (corresponding to λ = 1.0 Nm/degree for q = 40) and Fql, etc. = 8*5 N is necessary.

The posture-activity diagram for loadcase 2 and t = 0.5 is presented in Figure 7-12. From the diagram it is seen that the minimum value of a is about 32 mm for λ_{so} = 3.6 and about 36 mm for λ_{so} = 1.8 Nm/degree. To maintain lateral stability at these a-values, a minimum local lateral support equivalent to λ = 1 Nm/degree (Fit = 2*11.2 N) and Fql,etc. = 8*5 N is necessary.

The influence from the the relative lordosis on the posture-activity diagram is shown in Figure 7-12. The diagrams for t = 1.0, λ_{so} = 1.8 Nm/degree and t = 0.5, λ_{so} = 3.6 Nm/degree are shown. For both diagrams, the local lateral support is Fit = 10*11.2 N ($\Delta\lambda$ = 1 Nm/degree for q = 40) and Fql, etc. = 8*10 N. From the figure it is seen that t = 1.0 gives a slightly higher lateral stability and a slightly lower critical global muscle activity α_c compared to t = 0.5. The minimum a-value set by the condition for sagittal stability is about 31 mm for t = 1.0 and about 32 mm for t = 0.5.

Loadcase 3. Upper-body weight plus 1000 N extra vertical load carried on the shoulder

In this case the load is the combination of the gravity load acting at the center of gravity of the upper body (as before assumed to be placed 175 mm above the T12-L1 disk-midpoint) and the outer load attached at the shoulders (at a height of 290 mm). The resulting force of 1370 N acts at a height of 259 mm.

The complete stability diagram for t = 0.5 is shown in Figure 7-14. The mechanical behavior of the system is essentially the same as for the loadcases 1 and 2. From the figure it is seen that a minimum local lateral stabilization corresponding to Fit = 10*11.2 N (corresponding to a lateral stability of λ = 1.0 Nm/degree) and Fql, etc. = 8*10 N is necessary to fulfill the conditions for lateral stability for q = 40 at the given a-value of 42.5 mm. The condition for sagittal stability demands a q-value of about 38.

For t = 0.3, the conditions for lateral stability lie very close to those for t = 0.5 (the difference is not visible on the scale to which the diagram is drawn).

The sagittal stability diagram for t = 0.5 (λ_{so} = 3.6 and 4.5 Nm/degree) and t = 0.3 (λ_{so} = 4.5 Nm/degree) is shown in Figure 7-15. The characteristics lie very close to each other which indicate that the stability conditions only to a small degree are influenced by the relative lordosis t and the passive flexion stiffness λ_{so}.

Figure 7-16 shows the posture-activity diagram for loadcase 3 and t = 0.5. From the diagram it is seen that sagittal stability is obtained for an a-value greater than about 40 mm for λ_{so} = 3.6 Nm/degree (best choice) and an a-value greater than about 42 mm for λ_{so} = 1.8 Nm/degree (soft back). The activity in the local lateral stabilizing system is Fit = 10*11.2 N (corresponding to lateral stiffness λ = 1.0 Nm/degree) and Fql, etc. = 8*10 N.

The posture-activity diagrams for t = 0.5 and t = 0.3 are shown in Figure 7-17.

From the figure it is seen that the condition for sagittal stability give minimum a-values for which stability prevails of about 40 mm for both t = 0.5 and t = 0.3.

From the stability curves for loadcases 1, 2 and 3,

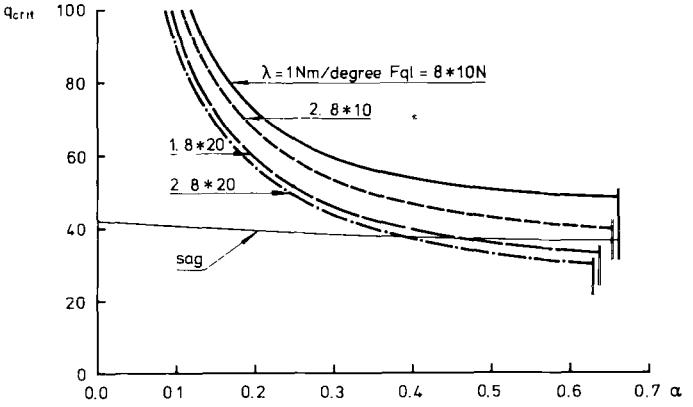

Figure 7-14. Complete stability diagram for loadcase 3: upper body weight plus 1000 N carried on the shoulders for relative lordosis t = 0.5 and a = 42.5 mm. Lateral stability is shown for Fit = 10*11.2 and 10*22.4 N (corresponding to a lateral stiffness λ = 1.0 and 2.0 Nm/degree), Fql, etc. = 20 and 40 N. λ_{lo} = 1.3 and λ_{ro} = 13 Nm/degree. Sagittal stability is shown for λ_{so} = 3.6 Nm/degree and cmf = 0.5. The influence on the sagittal stability from Fit and Fql, etc. is very small and is not visible on the scale to which the diagrams are drawn. Each line terminates at $\alpha = \alpha_c$.

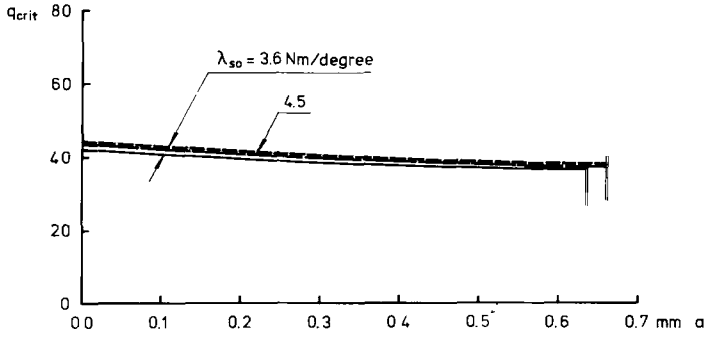

Figure 7-15. Sagittal stability for loadcase 3: a = 42.5 mm, dashed lines: t = 0.5, λ_{so} = 3.6 and 4.5 Nm/degree. Full drawn line: t = 0.3, λ_{so} = 4.5 Nm/degree. Fit = Fql, etc = 0. Each line terminates at $\alpha = \alpha_c$.

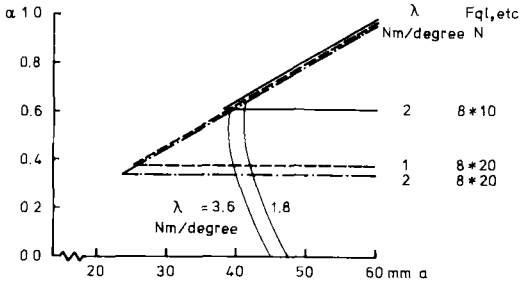

Figure 7-16. Posture-activity diagram for loadcase 3, q = 40 and t = 0.5. Sagittal stability: λ_{so} = 1.8 and 3.6 (best choice) Nm/degree, cmf = 0.5. Local lateral stabilization: Fit = 10*11.2 and 10*22.4 N (corresponding lateral stiffness λ = 1.0 and 2.0 Nm/degree), Fql, etc. = 20 and 40 N, λ_{lo} = 1.3 and λ_{ro} = 13 Nm/degree.

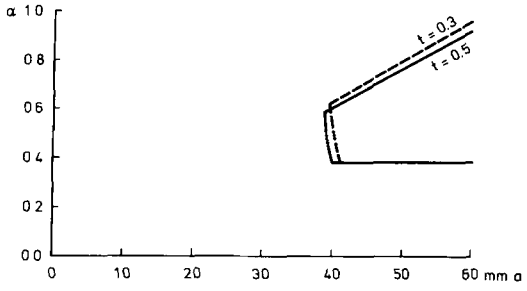

Figure 7-17. Posture-activity diagrams for loadcase 3. Comparison of conditions for t = 0.5 and t = 0.3. Full drawn lines: t = 0.5, λ_{so} = 3.6 Nm/degree, dashed lines: t = 0.3, λ_{so} = 4.5 Nm/degree, cmf = 0.5, Fit = 10*11.2 N (λ = 1 Nm/degree), Fql, etc. = 8*20 N, λ_{lo} = 1.3 and λ_{ro} = 13 Nm/degree.

the conditions for stability concerning activity in the global and local systems and for minimum a-values are found. No restrictions can however be made for the magnitude of the value of the relative lordosis t.

Muscle stress

In order to further investigate possible postures and muscle activities during standing, muscle stress in the global and the local systems are calculated for the three loadcases. The global muscle stress for $\alpha = \alpha_c$ is calculated according to eqn. 6.11 using the minimum value of α_c at which stability can be obtained for the cases shown in Figures 7-10 (loadcase 1), 7-13 (loadcase 2) and 7-17 (loadcase 3). The muscle stress at the L5-S1 level in the local sagittal system, i.e. the multifidi- and interspinal muscles, is calculated according to 6.45 for the same cases using $\Phi = 2.5$ degrees for loadcases 2 and 3 and $\Phi = 0$ degrees for loadcase 1. In addition, muscle tensions are calculated for intermediate t-values (not reported elsewhere in this work). The global and local muscle tension diagrams are shown in Figure 7-18 as a function of the relative lordosis t.

The muscle stress shall be compared to the physiological limit. For biceps brachii, the maximum strength is reported to lie in the range 0.4 - 0.8 MPa with a mean value of 0.63 MPa (Ikai and Fukunaga 1968). See further page 37.

From the diagrams, the following conclusions can be drawn:

1. The maximum local sagittal muscle stress σ_l varies almost linearly with t and may reach values of the same order as the physiological limit for loadcases 2 and 3.
2. The global muscle stress mainly depends on the loadcase and only weakly on t.
3. For loadcases 1 and 2, the local muscle stress are greater than the global muscle stress.
4. For loadcase 3, the local and the global muscle stress are close to each other for $t \approx 0.3$. For t greater than this value, the local muscle stress is greater than the global muscle stress.
5. For loadcase 1, the muscle stresses are well below the physiological limit.

Since $\alpha \leq \alpha_c$ the highest possible stress in the global erector spinae muscle for a fixed value of a is:

$$\sigma_g = \alpha_c Q / A_g \qquad (7.1)$$

The minimum value of α_c for a stable equilibrium depends on several factors. The most important one seems to be the load magnitude (Q). Other factors of importance are the forces in the local lateral system,

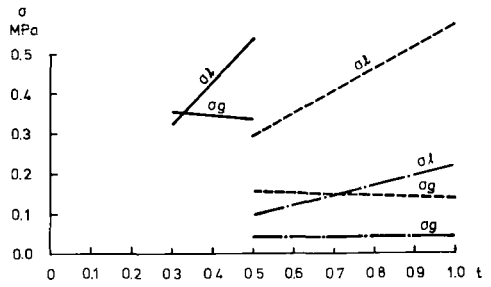

Figure 7-18. Global (g) and local (l) muscle tensions for loadcase 1 (dashed-dotted lines), loadcase 2 (dashed lines) and loadcase 3 (full drawn lines) as a function of the relative lumbar lordosis t. The corresponding minimum distances of a for each loadcase are 17.5 - 21 mm for loadcase 1 (Figure 7-10), 32 - 33 mm for loadcase 2 (Figure 7-13) and about 40 mm for loadcase 3 (Figure 7-17).

i. e. the the quadratus lumborum, the local fibers of the erector spinae muscles and the intertransverse muscles. Different degree of the lumbar lordosis also plays a part.

Increase of the posture parameter a increases α_c considerably. In fact, α_c is found to increase linearly with a.

In the cases studied the minimum value of α_c is found to vary between about 0.2 (for a case belonging to loadcase 1) and about 0.67 (for a case belonging to loadcase 3). For each loadcase, however, the relative variation of the minimum value of α_c is very small, of the order of $\pm$ 10 % in the parameter interval studied.

For one and the same loadcase and value of a, the maximum stress σ_l in the muscles belonging to the local sagittal system decreases when α increases, as could be expected. Thus the smallest stress is obtained at $\alpha = \alpha_c$. Consequently, if $\sigma_l < \sigma_g$ for $\alpha = \alpha_c$, the smallest maximum muscle stress is obtained for some $\alpha < \alpha_c$ at which $\sigma_l = \sigma_g$.

However, as shown in Figure 7-18, the value of σ_l depends strongly on the relative lumbar lordosis t, whereas σ_g is only weakly dependent on t. Therefore, if $\sigma_l > \sigma_g$ the lumbar lordosis can in principle be diminished until $\sigma_l = \sigma_g$.

The discussion shows that appropriate adjustment of α (the activity in the global system) and of t (the lumbar lordosis) can be used to minimize the maximum stress in the system. If the distance a is increased, for example by flexing the trunk, whereas α is kept constant (*i.e.* σ_g is constant), then σ_l increases. Calculations for loadcase 3, starting with $\alpha = \alpha_c$ and with t = 0.3, show that σ_l increases by 0.1 MPa when a increas-

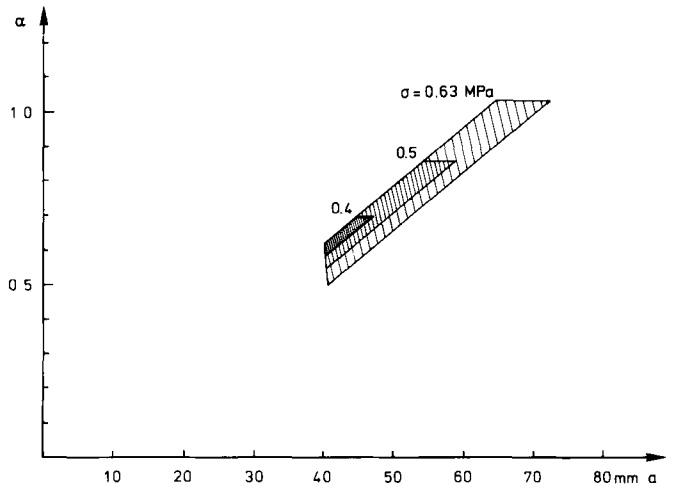

Figure 7-19. Posture-activity diagram for loadcase 3. t = 0.3, Fit = 10 * 11.2 N, Fql, etc. = 8 * 20 N and best choice parameter set. The shadowed areas show allowed a-α combinations for tension limits of 0.4, 0.5 and 0.63 MPa. In addition to the three limits earlier obtained in the posture-activity diagrams (based on equilibrium and stability reasons), there is one upper limit on α from the condition for the global muscle tension and one limit almost parallel to the α_c-line from the condition for local sagittal muscle tension.

es by about 2.5 mm. However, the increase of σ_l, calculated in this way, is probably somewhat exaggerated, since the same principles for the force distribution introduced to make the system statically determinate, were assumed. Now, with decreasing α the freedom of choice of the equilibrium state increases. Another force distribution could probably give rise to a smaller increase of σ_l. Hence the distance a can probably be allowed to increase more than 2.5 mm, perhaps a few mm, without increasing σ_l more than about 0.1 MPa.

The discussion together with the qualitative results shown in Figure 7-18 for $\alpha = \alpha_c$, shows that the maximum muscle stress can be unacceptably high for small α and large a within the stability region. Hence the whole stability region cannot be used, at least not at high loads. If one assumes a certain physiological limit of the muscle stress, then it is obvious (see eqn. 6.11) that σ_g is unacceptably high above a certain α-value. This fact, together with the fact just discussed, that σ_l becomes unacceptably high if the distance a exceeds a certain value, dependent on α, leads to a permissible region in the posture-activity diagram. For loadcase 3, using three values for the stress limit, this is shown in Figure 7-19. The limits are 0.4, 0.5 and 0.63 MPa. The latter value is the mean value for maximum strength of biceps brachii found by Ikai and Fukunaga (1968), see further page 37.

Posture change for increased vertical loading

From the diagrams in the preceding sections, it is found that two posture parameters, the distance a and the relative lordosis t, are important.

Sagittal stability of the system demands a minimum a-value. From Figures 7-2 (loadcase 1), 7-13 (loadcase 2) and 7-16 (loadcase 3) it is seen that the minimum a-value for which stability is possible increases from a ≈ 21 mm for loadcase 1 to a ≈ 32 mm for loadcase 2 and to a ≈ 40 mm for loadcase 3.

In order to avoid excessive local muscle stress, as the diagrams in Figure 7-18 indicate, increased vertical loading on the spinal system must be met by decreased magnitude of the relative lumbar lordosis t. Also a small flexion of the lumbar spine seems to be needed in order to minimize the maximum local muscle stresses at the upper and lower lumbar levels. Such a posture adjustment is probably automatically performed when a heavy load is carried. In the "optimal case" the changes in flexion and lumbar lordosis increase the distance a somewhat beyond the optimum value required to maintain stable equilibrium. The value of a, however, can of course be controlled independently of the posture by adjustment of the positioning of the load.

8. Discussion

The concept of stability

Very few works on the stability of the spinal system are presented in the literature.

The mechanical stability of the ligamentous spine was experimentally investigated by Lucas and Bresler (1961) who defined the buckling load with respect to *lateral* stability. With respect to flexion–extension the spine, however, as could be expected, did not show any typical buckling behavior, *i.e.* a sudden loss of equilibrium. Instead the sagittal deformations continuously increased at increased vertical loading. To be able to perform the lateral stability experiments, Lucas and Bresler had to restrict the sagittal deflections by means of two strings.

The characteristic mechanical quality of the spinal system (or any muscle-skeletal system) is that equilibrium is obtained at a specified posture. When the spinal system is subjected to an increasing vertical load, the induced deformations of the system are small (essentially compression and shear of the intervertebral discs). A change of posture is thus essentially an *active* measure, *i.e.* controlled by muscles, and only to a minor degree a result of passive deformations. Some posture changes, for instance flattening of the lumbar lordosis when carrying a heavy load, are clearly performed in order to avoid muscle overloading.

To be able to evaluate the mechanical stability of the spinal system, the stiffnesses of the passive components (motion segments) and the active components (muscles) must be taken into consideration.

A few theoretical works on spinal stability using beam models with passive properties, only, are described in the literature. These models, however, completely fail to describe the stability of the real system as no muscle stiffnesses are included.

Broberg (1981) has described a method to evaluate the stiffening influence from the muscles. The investigation presented here is partly based on his concept.

Delimitations

In the model, only back muscles and no abdominal muscles are included. In an experimental study on muscle activity in the standing posture, Asmussen and Klaussen (1962) found that about 75% of the subjects used only back muscles to counteract the gravity forces. The rest used mainly abdominal muscles which implies a somewhat different overall posture. Hence the model used in the present investigation corresponds to the behavior of the majority group.

The stability analysis was made for the lumbar spine, and the thoracic region was considered much stiffer than the lumbar region. There are three reasons for this: 1) the passive stiffnesses of the motion segments are about 50% higher for the thoracic region compared to the lumbar region (Markolf 1972); 2) the ribs, and thereby the whole ribcage, give mechanical support to the motion segments which furthermore increases the stiffness; 3) the local moments carried by the local system in the lower thoracic region are higher than corresponding moments in the lumbar region, which indicates that also the active stiffness of the thoracic region is higher. From the lumbar point of view the thoracic cage can therefore be considered as a rigid body. This definitely does not contradict the fact that the thoracic spine is far from stiff. The assumption of a rigid thoracic cage was used only in connection with possible deformation disturbances from an equilibrium state at a small range of load-postures.

The psoas muscle was not included in the model. The argument for this is that, as the main role of the psoas is to control the legs, stability of the lumbar spine shall be maintained independently of — or in some cases even in spite of — the use of the psoas. When standing, the psoas may anyway contribute to the stability. This should be taken into consideration when the theoretical results here are compared to experimental findings presented in the literature.

The latissimus dorsi muscles were not included either. No outer load is assumed to be transferred via the arms and consequently the assumption of silence in these muscles ought to be reasonable.

The study was limited to symmetric loading and symmetric postures. This is a starting point. For a more comprehensive understanding of the mechanical behavior of the spinal system a detailed study of non-symmetric cases is also important.

Comparison to experimental findings presented in the literature

The whole body gravity line falls approximately through the midpoint of L5 (During et al. 1985). As the

combined center of gravity of the abdominal viscera (the weight of the viscera is assumed to be carried directly by the pelvis) and parts below falls posterior to the whole-body gravity center, the upper body gravity center falls anterior to the midpoint of L5. About 75% (Asmussen and Klaussen 1962) of people studied used their back muscles during standing while the rest mainly used their abdominal muscles. The back muscle group were observed to have a slightly more forward leaning posture and this indicates that the gravity line for the back muscle group falls even somewhat more anterior. When 400 N vertical load was imposed a slight flexion of the thoracic cage and a flattened back was observed.

In investigations on the gravity line of the upper-body, different results are reported. The test was made by immersing the subject into water up to a midlumbar level and thus excluding the weight of the immersed parts as the density of the body is approximately equal to the density of water. Asmussen (1960) found the gravity line to fall about 20 mm anterior of the midpoint of L4 which is close to the result found in the present work. Klaussen (1965) and Klaussen & Rasmussen (1968), however, found the upper-body gravity line to fall about 15 mm posterior of L4. The figures in the latter investigations do not confirm the results found here. However, because of the very small moments involved in this loadcase, a number of explanations of this discrepancy is possible, for instance a small activity in abdominal or psoas muscles or passive moments due to a somewhat increased lumbar lordosis.

The theoretical model used here predicts that the muscle forces in the local sagittal system (the multifidi, the intertransverse and in the upper lumbar region also the spinalis muscles) is minimum at the L3-L4 disk-midpoint level. This minimum must, of course, be positive but can approach zero.

To be able to compare the theoretical results to EMG-measurements, estimates must be made concerning how the position of the electrodes is related to the different muscle groups defined in this work. The following relations are assumed to hold:

1. Surface electrodes placed 3 to 6 cm laterally to the spinous processes measure global erector spinae activity at L1 and L3 levels. At the L5 level they measure activity in the local sagittal system as there is no active part of the erector spinae muscle in this area. The global force at this level is carried by the erector spinae aponeurosis.
2. Wire electrodes in the multifidi muscles measure the muscle tension in the local sagittal system.
3. The EMG activity is an indicator of muscle force. Even at zero force there is, however, a certain electrical activity in the muscles. This level is low and can be estimated from EMG-registrations for a very relaxed posture.

Detailed measurements on the EMG-activity at different spinal levels during normal standing with no outer load have been performed by Andersson et al. (1974) and by Jonsson (1974). The results obtained in these investigations confirm the muscle force distribution found in the present study, i.e. minimum force at the L3-L4 level. The experimental findings also indicate that a certain force is carried by the local sagittal system at the L3-level during normal standing.

The only investigation on EMG-activity on different spinal levels for increased vertical loading in the standing posture found in the literature is the thesis by Jonsson (1970). The study, however, was performed on a few subjects only and no clear conclusion of EMG-activity distribution can be drawn.

Muscle stiffness

In the present work, the elastic behavior of a muscle-skeletal system is determined. The passive properties of the joints, *i.e.* the motion segment characteristics and the stiffnesses of the activated muscles are included. For increased vertical load, the need for stiffness to maintain stability is increased which implies contribution from the muscles as the passive stiffness properties cannot be controlled and remain essentially unchanged. It seems quite clear from investigations presented in the literature (Hoffer and Andreassen 1981, Hunter and Kearney 1982, 1983, Kearney and Hunter 1982, Morgan 1977, Rack and Westbury 1974, 1984) that the muscle stiffness increases with increasing muscle force and, at least for muscle stress well below the physiological limit, the stiffness is approximately proportional to the muscle force.

Subcritical stiffness

As mentioned in Introduction, the upright posture can, under certain circumstances, be maintained also for a mechanical system which is not inherently stable, by appropriate action of the muscles. This can be expected to occur if the system stiffnesses are only somewhat smaller than those needed because then a buckling attempt would proceed so slowly that there would be ample time for corrections. If this is the case, stability regions shown in the posture-activity diagrams in Chapter 7 should be somewhat, though not much, enlarged.

9. Summary

From the mechanical point of view the spinal system is highly complex, containing a multitude of components, passive and active. In fact, even if the active components (the muscles) were exchanged by passive springs, the total number of elements considerably exceeds the minimum needed to maintain static equilibrium. In other words, the system is statically highly indeterminate.

The particular role of the active components at static equilibrium is to enable a virtually arbitrary choice of posture, independent of the distribution and magnitude of the outer load albeit within physiological limits.

Simultaneously this implies that ordinary procedures known from the analysis of mechanical systems with passive components cannot be applied. Hence the distribution of the forces over the different elements is not uniquely determined.

Consequently nervous control of the force distribution over the muscles is needed, but little is known about how this achieved. This lack of knowledge implies great difficulties at numerical simulation of equilibrium states of the spinal system. These difficulties remain even if considerable reductions are made, such as the assumption that the thoracic cage behaves like a rigid body.

A particularly useful point of view about the main principles of the force distributions appears to be the distinction between a *local* and a *global* system of muscles engaged in the equilibrium of the lumbar spine. The local system consists of muscles with insertion or origin (or both) at lumbar vertebrae, whereas the global system consists of muscles with origin on the pelvis and insertions on the thoracic cage.

Given the posture of the lumbar spine, the force distribution over the local system appears to be essentially independent of the outer load of the body (though the force *magnitudes* are, of course, dependent on the magnitude of this load). Instead different distributions of the outer load on the body are met by different distributions of the forces in the global system. Thus, roughly speaking, the global system appears to take care of different distributions of outer forces on the body, whereas the local system performs an action, which is essentially locally determined (*i.e.* by the posture of the lumbar spine).

The present work focuses on the upright standing posture with different degree of lumbar lordosis. The outer load is assumed to consist of weights carried on the shoulders. By reduction of the number of unknown forces, which is done by using a few different principles, a unique determination of the total force distributions at static equilibrium is obtained. Different reductions of this kind are studied. One element of these reductions consists of the choice of the magnitude of the forces in the global system. Equilibrium can be maintained at different choices below a certain level. Generally speaking, smaller forces in the global system imply larger forces in the local system, as could be expected.

Another element of the reductions simply consists of excluding a large number of muscles, namely those believed to be rather silent at the load-postures studied. (Their function is obviously more pronounced at other load-postures.)

The equilibrium state thus found is not necessarily stable. In fact stability imposes severe restrictions on the possible equilibrium states.

The stability conditions are discussed in the usual way, *i.e.* by assuming an infinitesimal disturbance from the equilibrium state and then studying the change of mechanical potential energy of the system. This can be done by assuming that a configuration disturbance is accompanied by a unique change of the forces in the system, i.e. even the active components (the muscles) are assumed to react in a manner that depends only on their change in length. Thus, during the disturbance (which is supposed to take place within a time too short for conscious counteraction of the muscles) the muscles are assumed to behave in the same manner as a passive spring. Moreover, due to the smallness of the disturbance, this spring can be assumed to be linear. The stiffness, however, depends on the (equilibrium) force of the muscle.

Certain experiments indicate that the "passive muscle stiffness" to be used is proportional to the (equilibrium) muscle force. Thus a proportionality constant, the "muscle stiffness coefficient" is introduced. From the experiments the value of this coefficient can be estimated.

The stability conditions, that the potential change at any admissible infinitesimal disturbance from an equi-

librium state shall be positive, can be handled by powerful numerical methods even for fairly large systems. For the lumbar spine investigations have been made under different assumptions of the force distributions at equilibrium. The result indicates that stability prevails in a certain interval of such assumptions.

This means that a *possible* region of stability has been found. By making other assumptions a larger region could, perhaps, be found, but so many various assumptions were studied that the difference would probably be very small.

The calculations show that instability can occur under one of two possible kinds of disturbance configurations. One is simply flexion-extension (leading to sagittal instability). The other is a combination of lateral bending and axial rotation (leading to lateral–rotational instability).

Essentially the only requirement to ensure sagittal stability seems to be that the muscle stiffness coefficient is high enough.

Lateral–rotational stability appears to prevail if the forces in the global system are high enough. However an upper boundary exists above which equilibrium cannot be maintained. In addition some muscles of the local system, notably the quadratus lumborum together with certain local fibers of the erector spinae, must be sufficiently activated.

Some stabilizing influence from the thoracolumbar fascia was found, due to fact that it constrains the global erector spinae muscles laterally and sagittally with respect to the lumbar spine.

The implications of different degrees of lumbar lordosis were studied. They seem to be small as regards the stability. However, at higher loads there is a clear

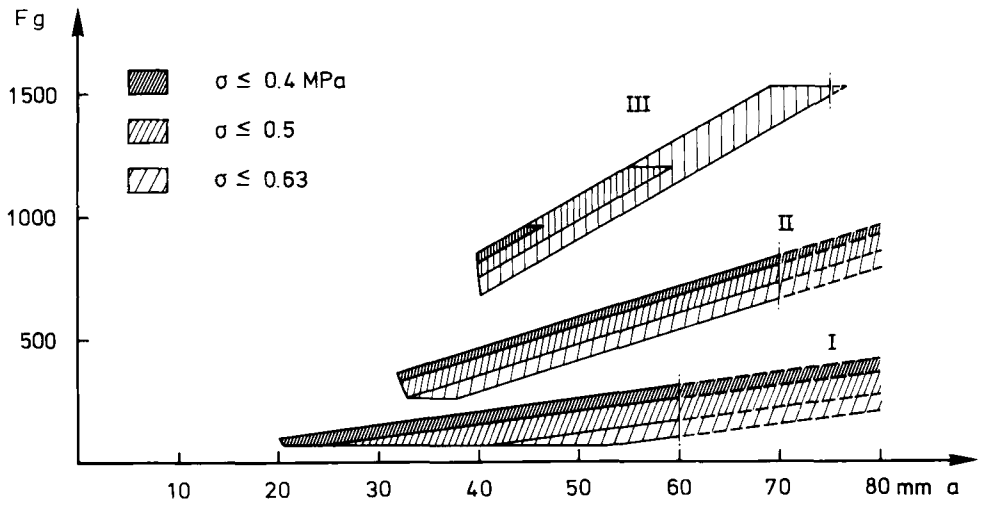

Figure 9-1. Possible permissible combinations of the distance a (position of the gravity line in relation to the most anterior disk-midpoint) and Fg, (the global erector spinae muscle force) at three different loadcases at upright standing. I: upper-body weight only, II: upper-body weight plus 400 N carried on the shoulders, III: upper-body weight plus 1000 N carried on the shoulders. The limits are given by conditions for stability, equilibrium and maximum permissible muscle tensions. Three different ranges of permissible muscle tensions are considered where the highest value (0.63 MPa) corresponds to the maximum strength (Ikai and Fukunaga 1968) and the lowest value (0.4 MPa) to a tension level that can be maintained for a few minutes. A flattening of the lumbar lordosis is assumed for loadcases II and III in order to avoid muscle overloading. The calculations are made for relative lumbar lordosis t = 1.0 at loadcase I, for t = 0.5 at loadcase II and for t = 0.3 at loadcase III.

The left limit for each loadcase is set by the condition for sagittal stability and the upper left limit is set by the condition for equilibrium. The other limits are set by the condition for maximum permissible muscle tension (except the lower horizontal limits of loadcases I and II which are set by the condition for lateral stability). The horizontal upper limit refers to the global erector spinae, whereas the slanting lower limit refers to the local muscles.

As the figure indicates, the permissible regions for loadcases I and II would extend far to the right, but the calculations have been carried out only to a = 60 mm (loadcase I), a = 70 mm (loadcase II) and a = 75 mm (loadcase III).

It should be observed how the permissible region shrinks with increasing load and with decreasing maximum permissible muscle tension.

relation between the lordosis and the muscle tensions. Thus the reduction of the lordosis, known to take place under heavy vertical loading, appears to be necessary in order to keep all muscle tensions at physiologically acceptable levels.

Consideration of muscle tensions leads to the result that not all states of stable equilibrium can be realized. In fact, at increased loading, a shrinking part of the region of stable equilibrium is compatible with physiological acceptable muscle tensions. Thus the range of possible postures labelled "upright standing" becomes successively restricted (towards a small lumbar lordosis, a certain narrow region of trunk flexion and a rather critical positioning of the weight) and the range of possible distribution of muscle forces becomes very small (tending towards forces in the global erector spinae close to the maximum allowable ones for equilibrium).

The results can be epitomized by the diagram in Figure 9-1, showing possible combinations of posture and global erector spinae muscle force under assumptions of a few maximum values of permissible muscle tensions. One observes how the possible posture-activity region becomes smaller when the load increases. Theoretically, it would be shrunk to a point at a certain load. However, an ample size of the region is, of course, needed, in order to provide leeway for variations of postures and muscle force distribution. Thus one could imagine that the aim is to center posture-activity to some optimum midpoint in the permissible region, and the deviations from this point are met by appropriate counteractions directed from some sophisticated control system.

10. References

Adams M A, Hutton W C, Stott J R R. The resistance to flexion of the lumbar intervertebral joint. Spine 1980;(5):245-253.

Adams M A, Hutton W C. The effect of posture on the role of the apophysial joints in resisting intervertebral compressive forces. J Bone Joint Surg 1980; (62B):358-362.

Andersson G, Jonsson B, Örtengren R. Myoelectric activity in individual muscles in sitting. A study with surface and wire electrodes. Scand J Rehab Med 1974;Suppl 3:91-108.

Andersson G, Örtengren R, Nachemson A. Intradiskal pressure, intra-abdominal pressure and myoelectric back muscle activity related to posture and loading. Clin Orthop 1977;(129):156-164.

Asmussen E. The weight-carrying function of the human spine. Acta Orthop Scand 1960;(29):276-290.

Asmussen E, Klaussen K. Form and function of the erect human spine. Clin Orthop 1962;(25):55-63.

Bendix T, Sorenssen S S, Klaussen K. Lumbar curve, trunk muscles, and line of gravity with different heel heights. Spine 1984;(9):223-227.

Bergmark A. Mechanical stability of the human lumbar spine. Thesis. Dept. of Solid Mechanics, Lund University, Sweden. Lund 1987.

Berksson M H, Nachemson A, Schultz A B. Mechanical properties of human lumbar spine motion segments - Part II: Responses in compression and shear, influence of gross morphology. J Biomechanical Engineering 1979;(101):53-57.

Bogduk N. A reappraisal of the anatomy of the human lumbar erector spinae. J Anatomy 1980;(131): 525-540.

Bogduk N, MacIntosch J. The applied anatomy of the thoracolumbar fascia. Spine 1984;(9):164-170.

Broberg K B. The mechanical behaviour of the spinal system. Report from the division of solid mechanics, Lund Institute of Technology, Lund Sweden, 1981.

Broberg K B. On the mechanical behaviour of intervertebral discs. Spine 1983;(8):151-165.

Crowninshield, R D, Brand, R A. A Physiologically based criterion of muscle force prediction in locomotion. J Biomechanics 1981;(14):793-801.

Dul J, Townsend M A, Shiavi R, Johnson, G E. Muscular synergism - I. On criteria for load sharing between synergistic muscles. J Biomechanics 1984a;17(9):663-673.

Dul J, Johnson G E, Shiavi R, Townsend M A. Muscular synergism - II. A minimum-fatigue criterion for load shearing between synergistic muscles. J Biomechanics 1984b;17(9):675-684.

During J, Goudfrooij H, Keesen W, Beeker Th W, Crowe A. Toward standards for posture. Postural characteristics of the lower back system in normal and pathologic conditions. Spine 1985;(10):83-87.

Grew N D. Intraabdominal pressure response to loads applied to the torso in normal subjects. Spine 1980;(5):149-154.

Hemborg B. Intraabdominal pressure and trunk muscle activity during lifting. Thesis. Department of Physical Therapy, University of Lund, Sweden. 1983.

Hoffer J A, Andreassen S. Regulation of soleus muscle stiffness in premammillary cats: Intrinsic and reflex components. J of Neurophysiology 1981; 45(2):267-285.

Hunter I W, Kearney R E. Dynamics of human ankle stiffness: Variation with mean ankle torque. J Biomechanics 1982;(15):747-752.

Hunter I W, Kearney R E. Invariance of ankle dynamic stiffness during fatiguing muscle contractions. J Biomechanics 1983;(16):985-991,.

Ikai M, Fukunaga T. Calculation of muscle strength per unit cross-sectional area of human muscle by means of ultrasonic measurement. Int Z angew Physiol einschl Arbeitsphysiol 1968;(26):26-32.

Jacob H A C, Suezawa Y. On the initiation of spondylolysis through mechanical factors. Biomechanics: Current Interdisciplinary Research. Martinus Nijhoff Publishers, Dordrecht 1985.

Jonsson B. The lumbar part of the erector spinae muscle. Thesis, Dept of Anatomy, University of Göteborg, Sweden. Göteborg 1970.

Jonsson B. Function of the erector spinae muscle on different working levels. Acta Morph Neerl-Scand 1974;(12):211-214.

Kearney R E, Hunter I W. Dynamics of human ankle stiffness: variation with displacement amplitude. J Biomechanics 1982;(15):753-756.

Klaussen K. The form and function of the loaded human spine. Acta Physiol Scand 1965;(65):176-190.

Klaussen K, Rasmussen B. On the location of the line of gravity in relation to L5 in standing. Acta Physiol Scand 1968;(72):45-52.

Langenberg W. Morphologie, physiologischer Quersnitt und Kraft des M. erector spinae im Lumbalbereich des Menschen. Z Anat Entwickl-Gesch 1970;(132):158-190.

Lucas D B, Bresler B. Stability of the ligamentous spine. Biomechanics Laboratory University of California. San Francisco Berkeley. Number 40, 1961.

Markolf K L. Deformation of the thoracolumbar intervertebral joints in response to external loads. J Bone Joint Surg 1972;(54A):511-533.

Morgan D L. Separation of active and passive components of short-range stiffness of muscle. Am J Physiol 1977;(232):45-49.

Nachemson A L, Schultz A B, Berksson M H. Mechanical properties of human lumbar spine motion segments. Influences of age, sex, disc level and degeneration. Spine 1979;(4):1-8.

Nachemson A L, Andersson G B J, Schultz A B. Valsalva maneuver biomechanics. Spine 1986;(11): 476-479.

Panjabi M M. Experimental determination of spinal motion segment behavior. Orthop Clin North Am 1977;8(1):169-180.

Panjabi M M, Brand R A, White A A. Mechanical properties of the human thoracic spine. J Bone Joint Surg 1976a;(58A):642-652.

Panjabi M M, Brand R A, White A A. Three-dimensional flexibility and stiffness properties of the human thoracic spine. J Biomechanics 1976b;(9): 185-192.

Panjabi M M, Krag M, White A A, Southwick W O. Effects of preload on load-displacement curves of the lumbar spine. Orthop Clin North Am 1977; 8(1):181-192.

Parnianpour M, Schechter S, Moritz U, Nordin M. Back muscle endurance in response to external load. 33rd annual meeting, Orthopedic Research Society, January 19-22, San Francisco, California, 1987.

Pope M H, Andersson G B J, Broman H, Svensson S, Zetterberg C. Electromyographic studies of the lumbar trunk musculature during the development of axial torques. 10th International Congress of Biomechanics. Umeå, June 15-20, 1985. Abstract Book. Arbete och Hälsa 1985:14.

Rack P M H, Westbury D R. The short range stiffness of active mammalian muscle and its effect on mechanical properties. J Physiology 1974;(240): 331-350.

Rack P M H, Westbury D R. Elastic properties of the cat soleus tendon and their functional importance. J Physiology 1984;(347):479-495.

Scholten P. Idiopatic Scoliosis. Thesis. Vrije Universiteit te Amsterdam. Amsterdam 1986.

Schultz A B, Andersson G B J, Haderspeck K, Örtengren R, Nordin M. Analysis and measurement of lumbar trunk loads in tasks involving bends and twists. J Biomechanics 1982a;(15):669-676.

Schultz A, Andersson G, Örtengren R, Haderspeck K, Nachemson A. Loads on the lumbar spine. J Bone Joint Surg 1982b;(64A):713-720.

Schultz A B, Benson D R, Hirsch C. Force-deformation properties of human costo-sternal and costovertebral articulations. J Biomechanics 1974;(7): 311-318.

Schultz A, Haderspeck K, Warwick D, Portillo D. Use of the lumbar trunk muscles in isometric performance of mechanically complex standing task. J Orthopedic Research 1983;(1):77-91.

Schultz A B, Warwick D N, Berksson M H, Nachemson A L. Mechanical properties of human lumbar motion segments - Part I: Responses in flexion, extension, lateral bending and torsion. J Biomechanical Engineering 1979;(101):46-52.

Skogland L B, Miller J A A. On the importance of growth in idiopatic scoliosis. Thesis. University of Oslo, Norway. 1980

Schmorl G, Junghans H. The human spine in health and disease. 2nd English edition. Stuttgart, Georg Thieme Verlag, 1968.

Sobotta J. Atlas of Human Anatomy. 8th Engl. edition by Frank H.J. Figge. Vol I. Hafner Publishing Company, INC., New York 1968.

Taylor J R, Twomey L T. Age changes in lumbar zygapophyseal joints. Spine 1986;(11):739-745.

White A A, Panjabi M M. Clinical biomechanics of the spine. Philadelphia Toronto, J.B.Lippincott Company 1978.